

# **Fractal Dimension Analysis to Facilitate Histopathology Diagnosis in Oral Carcinogenesis**

BY

SREE POORNIMA RAGHURAM  
B.E., Visveswaraya Technological University, India, 2010

THESIS

Submitted as partial fulfillment of the requirements  
for the degree of Master of Science in Bioengineering  
in the Graduate College of the  
University of Illinois at Chicago, 2013

Chicago, Illinois

Defense Committee:

Joel. L Schwartz, Chair and Advisor, College of Dentistry  
Guy Adami, Oral Medicine, College of Dentistry  
Michael Strosio

## **ACKNOWLEDGEMENTS**

I would like to thank my advisor, Dr. Joel L. Schwartz for his support and guidance throughout my research work. He has been the backbone of this project, and has been the most important reason to have been able to complete my thesis work. Along with Dr. Schwartz, his lab members have also provided a great deal of support with providing staining and tissue samples.

I would also like to thank former graduate student Yajur Parik, whose previous studies based on similar lines gave me much more clarity with my work. I would also like to thank him for taking his time out to discuss his project with me.

Last, I would like to thank my Department. Friends and family who have always supported me in my work and any decisions I have taken.

Thank You!

# **TABLE OF CONTENTS**

CHAPTER .....	PAGE
1. INTRODUCTION	
1.1. ORAL SQUAMOUS CELL CARCINOMA & ORO-PHARYNGEAL CARCINOMA .....	1
1.2. EPITHELIAL HISTOLOGY MARKERS.....	3
1.2.1. Epithelial Cell Size Change.....	5
1.2.2. Cell DNA .....	5
1.2.3. Epithelial-Epithelial Cell Bridges: Anaplasia .....	5
1.2.4. Differentiation .....	6
1.2.5. Growth.....	6
1.3. MESENCHYMAL HISTOLOGY MARKERS .....	7
1.3.1. Blood Cells .....	7
1.3.2. Stromal Cells.....	9
1.4. HISTOLOGY CHANGES IN PRE-MALIGNANT AND MALIGNANT DIAGNOSIS .....	10
1.5. GRADING & EVALUATION OF HISTOPATHOLOGICAL TISSUES .....	12
1.5.1. Brandwein histological model .....	15
1.5.2. Diagnostic assessments of Dysplasia .....	18
1.6. ENVIRONMENTAL FACTORS AFFECTING OSCC.....	18
1.6.1. Age .....	18
1.6.2. Ethnicity.....	20
1.6.3. Habits .....	20
1.6.4. Immunosuppression.....	22
1.7. IDENTIFICATION USING IMMUNOHISTOCHEMISTRY.....	23
1.7.1. Standard Approach .....	23
1.7.2. Protein Interactions of Immunohistochemistry.....	24
1.7.3. Fixation.....	25
1.7.4. Types of IHC Methods .....	25

1.7.5. Method of Staining using IHC methods .....	26
1.7.6. Advantages of IHC methods .....	26
1.7.7. Immunohistochemistry (IHC) in cancer.....	26
1.8. FRACTAL DIMENSIONS .....	27
1.8.1. History .....	27
1.8.2. Fractal geometry .....	27
1.8.3. Frac-Lac Plug-in.....	29
1.8.4. Fractal geometry and Cancer .....	29
1.9. ORAL CARCINOGENESIS ANIMAL MODELS .....	31
1.9.1. Need for Models.....	31
1.9.2. Advantages of Animal Models .....	31
1.9.3. Disadvantages .....	32
1.9.4. Hamster Model in OSCC .....	32
1.9.5. Rat/Mouse Model in Oral Carcinogenesis .....	35
1.9.6. Animal model used in this study .....	35
1.10. CHEMICAL CARCINOGENESIS .....	36
1.11. CANCER STEM CELLS.....	39

## **2. METHODS**

2.1. ORAL CARCINOGENESIS MODEL .....	41
2.2. HISTOPATHOLOGY ASSESSMENT.....	41
2.3. DETERMINING PATTERNS OF INVASION (POI) .....	42
2.4. TISSUE SELECTION AND NUMBER .....	43
2.5. FRACTAL DIMENSION ANALYSIS .....	44
2.5.1. SIMPLE BOX COUNT .....	45
2.5.2. INFLAMMATORY INFILTRATE ANALYSIS.....	46
2.6. IMMUNOHISTOCHEMISTRY.....	47
2.7. DATA ANALYSIS.....	48

### **3. RESULTS**

3.1 RATIONALE .....	51
3.2. EXPERIMENTAL ORAL CARCINOGENESIS MODEL .....	51
3.3. HISTOPATHOLOGY CRITERIA FOR ASSESSMENT OF PATHOLOGY .....	52
3.4. ORAL EPITHELIAL MUCOSA ARCHITECTURE CHANGES DURING CANCER .....	52
3.5. CONVERSION OF HISTOPATHOLOGY TO A FRACTAL DIMENSION ANALYSIS .....	53
3.6 A SERIES OF COMPARISONS WERE USED TO TEST ACCURACY OF FD ANALYSIS .	54
3.6.1 FD Analysis to Assess Difference between Identical Sets of Tissue images .....	57
3.6.2. Inflammatory Infiltrate and Brandwein Criteria.....	62
3.6.3. Assessment of Fractal Dimension (FD) Pattern, Lacunarity Characteristic .....	64
3.6.4. Assessment of Variability of FD Analysis with Lacunarity .....	66
3.6.5. Inter-Data Differentiation of the stages of Cancer development: Set 3 .....	69
3.6.6. Fractal Dimension Analysis in Immunohistochemistry Stained Tissue Sections.....	70

### **4. DISCUSSION**

4.1. SUMMARY OF RESULTS .....	77
4.2. INNOVATION.....	77
4.3. CONSISTENCY & REPEATABILITY .....	77
4.4. SENSITIVITY .....	80
4.4.1. Comparison of Stem cell markers.....	81
4.4.2. Stem Cell Markers to enhance Sensitivity .....	82
4.5 ENHANCING DIAGNOSTIC TOOL KIT .....	82

### **5. CONCLUSION.....**

### **6. FUTURE AIMS .....**

### **7. REFERENCES .....**

### **8. VITAE .....**

## **LIST OF FIGURES**

**Figure 1:** DBP Induced Cancers in Golden Syrian Hamster

**Figure 2:** A Modification of Brandwein's Patterns for Invasion for (POI) OSCC

**Figure 1:** Conversion process of digital slides through steps: 1, original image; 2, greyscale; 3, threshold to emphasize epithelial layer, POI circled in red.

**Fig 4:** Fractal Analysis: Multiple variable graphs of Test 1 and Test 2

**Figure 5:** The graph shows an insignificant difference of 0.0095 between the Fractal dimension values from Test 1 and Test 2.

**Figure 6:** Correlation (Test set 1 and Test set 2) of Total area of the infiltrate and Area fraction with the POI

**Figure 7:** Scatter plot with Fractal dimension (Simple box count) Vs Lacunarity (Simple box count) grouped with respect to POI

**Figure 8: Test set 3 data**

**Fig8 (a):** Inflammatory infiltrate scatter plot with total area plotted against area fraction

**Fig8 (b):** Spearman correlation scatter plot with Lacunarity versus Fractal dimension to determine their relation with POI.

**Fig 9:** Test set 2- Comparison between Stages during Oral Carcinogenesis

**Figure 10:** The difference in fractal dimensions with the addition of stem cell markers can be observed. The FD values increased with the markers.

**Figure 11:** Comparison of Contiguous sections & Non-contiguous sections stained with Stem cell marker CD44

## **LIST OF TABLES**

**Table 1:** DBP treated Group (Test Group 1)

**Table 2:** DBP treated Group (Test Group 2)

**Table 3(a):** T-test (assuming equal variances) for OSCC

**Table 3(b):** T-test (assuming equal variances) for OSCC

**Table 3(c):** T-test (assuming equal variances) for Dysplasia

**Table 4:** Inflammatory Infiltrate data for Test set 2

**Table 5:** T-test (assuming equal variances) for Inflammatory Infiltrate Data from Test 2

**Table 6:** DBP Treated Group (Test set 3)

**Table 7:** Independent T-test results for Test set 2 and Test set 3

**Table 8:** Inter-data T-test for Test set 3: Analysis between difference stages of cancer development

**Table 9:** PCNA Marker (Marker 1)

**Table 10:** Distinguishing the Normal tissues from Mild dysplasia, Mild dysplasia from Moderate dysplasia and Moderate dysplasia from severe dysplasia by the addition of PCNA (nuclear marker).

**Table 11:** Comparison of CD44 Contiguous sections & Non-contiguous sections stained with Stem cell marker CD44

**Table 12:** Paired sample t-test for determining significant contiguous tissues with PCNA and CD 44 markers.

**Table 13:** Marker 3: MAPK Expression

**Table 14:** Marker 3: 8-oxo-dG

**Table 15:** Comparison of markers

**Table 16:** Independent T-test for analysis of difference between the effects of markers

## **ABBREVIATIONS**

DBP	Dibenz [a, l] pyrene
FD	Fractal dimension
HNSCC	Head and neck squamous cell carcinoma
HPV	Human papilloma virus
OSCC	Oral squamous cell carcinoma
PAH	Poly-cyclic aromatic hydrocarbons
IHC	Immunohistochemistry
POI	Pattern of tumor invasion
ROI	Region of interest
II	Inflammatory Infiltrate



## **ABSTRACT**

**Background:** Oropharyngeal and Oral squamous cell carcinoma (OSCC) are diagnosed in approximately 270,000 patients worldwide. Diagnosis usually depends on assessment of tumor invasion patterns thus leading to differences in opinion between pathologists and reducing treatment effectiveness and ultimately survival.

**Objective:** We test the hypothesis that mathematical pattern recognition characterized by fractal dimension (FD) pattern analysis can improve histopathology diagnosis accuracy for OSCC. To accomplish this goal we combined digitalized, public domain software with recognized pathology criteria. We obtained an analysis of patterns of invasion (POI), inflammatory infiltration (II) and a selection of specific cells forming a FD pattern using immunohistochemical (IHC) noted protein expressions.

**Experimental method:** To accomplish FD analysis we used an experimental oral carcinogenesis Golden Syrian hamster (25 animals per groups: 4-5 wks of age) tumor model was induced with dibenz [a, l] pyrene (DBP) (0.0025 mM dissolved in acetone (1.0%, v/v); 2.5 nM/application to the floor of the mouth and lateral border of the tongue) and an application control (1.0% acetone). Accuracy was assessed by comparison of FD+/-POI;+/-II;+/-Lacunarity;+/-IHC: Test set 1 and Test set 2 which were obtained from 125 photographic images (20X magnification) a Test set 3 for IHC analysis used 70 images. Test set 3 tested enhancement of FD after tagged basal/supra basal keratinocyte populations using markers (proliferating cell nuclear antigen (PCNA); CD44; p38 mitogen activated phosphokinase (MAPK), and 8-Hydroxy-2'-deoxyguanosine) in contiguous and non-contiguous tissue sections were identified.

### **ABSTRACT (CONTD)**

Analysis was performed using Java-based image processing tool, ImageJ, which provided the Fractal dimensions (FDs) for each studied element. Statistical analysis such as spearman correlation and Kappa value analysis were also performed.

**Results:** FD analysis enhanced the accuracy with insignificant variability of diagnosis between normal, premalignant and malignant tissues using two independent examinations or repeated examination by an identical investigator. Furthermore inclusion of IHC enhanced FD analysis when markers identified cells with a significant contribution to the FD pattern using contiguous tissue sections.

**Conclusion:** FD analysis should be considered for improved diagnosis and understanding of experimental oral carcinogenesis tissues and this study provides a template to study human tissues to determine improved accuracy.

# **1. INTRODUCTION**

## **1.1. ORAL SQUAMOUS CELL CARCINOMA & ORO-PHARYNGEAL CARCINOMA**

Head and neck cancer is the sixth most common human cancer, representing 3% of all types of cancer. About 90% of all head and neck squamous cell carcinoma (HNSCC) are oral squamous cell carcinoma (OSCC). More than 300,000 new cases of oral squamous cell carcinoma are diagnosed annually.(Tanaka, Tanaka et al. 2011). They are characterized by abnormal and uncontrolled growth of cells, mainly through ability to invade tissues and organs, eventually disabling the functionality of the organ leading to death. (Krishnan, Venkatraghavan et al. 2012).

Accurate diagnosis of precancerous lesions and invasive carcinoma is needed because with greater accuracy our expectation is to reduce incidence of cancers with appropriate treatment at the appropriate time. (Mognetti, Di Carlo et al. 2006).Furthermore, a high rate of morbidity and mortality are attributed to late stage diagnoses that were not recognized or correctly evaluated during the diagnostic examination. In addition, late diagnosis for OSCC also contributes to risk for more metastatic sites and increased risk for primary malignant tumor and secondary growth expansion from an original primary OSCC. (Driemel, Kunkel et al. 2007)

Furthermore, there are recognized variations in diagnosis accuracy between trained pathologists and for inter-individual variability for premalignant or OSCC diagnosis. (Yadav KS (2012))(Sawair FA (2003))

This project was established to develop an innovative approach to improve diagnostic assessment and it expected to improve immediately our accuracy for diagnosis and late enhance clinical survival and/or response to treatment; once implemented during standard diagnostic examination.

Diagnosis is largely based on pattern recognition and assignment after attaining information for clinical behavior and presentation for an OSCC lesion. A diagnostic process therefore relies on recognizable changes in tissues that compose a cancer mass in conjunction with other modalities such as physical, hematologic examinations and radiology, to understand the quality and quantity of tissue damage and distribution.

In this cancer, oral squamous cell carcinoma; to achieve an accurate diagnosis we require a capability to dissociate pre-malignant and malignant tumor mass changes through use of accurate histopathology.

Histology examination requires a systematic approach to maintain diagnostic accuracy. Often with a comparison to normal tissue of the identical type, there are a complex variety of histology criteria that record changes in epithelium, mesenchymal stroma, and the structures and cells peculiar to OSCC. Histology diagnosis uses this variety to record recognizable changes in the epithelium and mesenchymal stroma.

The epithelium forms the oral mucosa and is a target tissue for malignant phenotypic change.

## **1.2. EPITHELIAL HISTOLOGY MARKERS**

### **Oral mucosa**

Although the general architecture from one anatomic site to another is very similar there are differences in regards to physiology, function, and basic cell biology such as cell turnover, expression of susceptibility genes, and type and composition of microbiome that sits on the mucosa. This variability in form and function is amplified during oral carcinogenesis and is exemplified by enhanced risk for one anatomic site compared to another. For example, common sites for moderate to severe dysplasia and OSCC are lateral border of the tongue, base of the tongue and floor of the mouth.

For this reason repeated presentation of premalignant and malignant changes in selected tissue sites offers an advantage for improving diagnostic accuracy.

Layers of normal oral mucosa Include:

**Stratum basale** is the basal layer forming the deepest of the epidermis. They consist of a single layer of columnar and cuboidal keratinocytes which act as the stem cell undergoing division to form the keratinocytes of stratum spinosum. In addition to the keratinocyte populations other cell types comprise melanocytes (pigment producing cells), Langerhans cells (immune cells) and merkel cells (touch receptors). The basal lamina is at the interface of the epithelium and lamina propria.(Shafer and Waldron 1975).

**Stratum spinosum:** A layer of epidermal cells found between the stratum granulosum and stratum basale. This layer contains keratinocytes and Langerhans cells.

The stratum basale and the first layers of the stratum spinosum are referred to as stratum germinativum because these cells give rise to new epithelial cells.

**Stratum granulosum** comprises of cells that are flat and about three to five layers thick. They are present in keratinized epithelium which helps in the formation of keratin complex.

**Stratum corneum** is the outermost layer of the epidermis mostly composed of corneocytes (dead cells) which lack nuclei and organelles.

Connective tissues are differentiated as Lamina propria and submucosa.

**Lamina propria** is the connective tissue layer just below the epithelium which is divided into papillary layer and reticular layer. The papillary layer forms finger like projections of connective tissue that extend deep in the epithelial layers. Lamina propria consists of blood vessels and fibroblasts, cells of blood vessels and lymphatics. The metabolic needs of avascular epithelium are sufficed by the vessels of the lamina propria (Squier and Kremer 2001).

**Rete pegs** are histological markers which are characterized by epithelial extensions that project into the underlying connective tissue in the mucous membranes. In the oral cavity, the attached gingiva to the epithelium of the mouth exhibit rete pegs. They are also termed as rete processes or rete ridges.

During oral carcinogenesis and presentation of characteristics noted below, the layers of epithelial oral will undergo change as normal changes to premalignant-dysplasia to malignant-OSCC.

### **1.2.1. Epithelial Cell Size Change:**

Pleomorphism can be used to describe the variability in size, shape or nuclei. They characterize malignant neoplasm and metaplasia. Malignant tissues form morphological and functional changes because of lack of differentiating cells leading to pleomorphism. Pre-malignant analysis of oral squamous cell carcinoma is usually carried out by assessing changes in nuclear and cellular size and shape. Evaluation of pleomorphism is more reliable to assess lesions and tumors on the tissues as malignant. Proliferation can be assessed by counting cells with labeled DNA, Studying nuclear morphology and nucleolar organizing regions, nuclear antigens and oncology encoded proteins. (Christopher and Mary 2001)

### **1.2.2. Cell DNA**

Hyperchromatism is a characteristic pathological marker which suggests a hyperchromatic state of nucleus .i.e. malignancy. It is depicted by abundance of DNA, excessive pigmentation, degeneration of cell nuclei which become filled with chromatin particles.

### **1.2.3. Epithelial-Epithelial Cell Bridges: Anaplasia**

Malignant neoplasm composed of undifferentiated cells is called anaplastic and the condition is termed as anaplasia. Lack of differentiation .i.e. anaplasia is the hallmark of malignancy. Anaplastic cells display pleomorphism with variable nuclei and bizarre size and shape. They grow in sheets with loss of interlinking structures and usually fail to develop recognizable patterns of orientation to one another. Anaplastic cells are

extremely hyperchromatic resulting in dark staining, and increased nuclear-to-cytoplasmic ratio.

#### **1.2.4. Differentiation**

**Hyperkeratosis** is the condition which occurs when the stratum corneum of the epidermal layers thicken, producing a qualitatively abnormality amount of keratin and an increase in the granular layer. Cornium layer normally varies in thickness so minor degrees of hyperkeratosis are difficult to assess. This condition usually is associated with lesions of the mucous membrane such as leukoplakia but it occurs in non-premalignant and premalignant types, and malignant conditions. (Chiang, Lang et al. 2000)

#### **1.2.5. Growth**

##### **Mitotic figure**

Mitotic counting is an important feature for grading malignancy. The condensed chromosomes by which a cell can undergo mitosis can be identified to define a mitotic figure. The aggregation of the chromosome during any of the stages of mitosis can be observed under the microscope. Some criteria to observe the mitotic figures are: Absence of nuclear membrane zone, Absence of a clear zone in the center or the presence of a hairy projection can be counted as mitotic figures. Structures without distinct mitotic figures should not be taken into consideration.(Reibel 2003)



Moreover, it is recognized to evaluate mitotic figures requires a rigid protocol to obtain an accurate analysis for this characteristics (Yadav KS, Gonuguntla S (2012)).

### **Hyperplasia**

It is the most common preneoplastic response to stimulus characterized by an increase in the number of cells. This in turn may result in enlargement of an organ leading to neoplasia. Hyperplasia is a physiological response to stimuli with the hyperplastic cells with subject to normal regulatory control mechanisms. Hyperplasia is induced due to number of stimuli such as proliferation of basal layer of the epidermis, chronic inflammatory response, and hormonal dysfunctions.(Bánóczy 1984)

### **Acanthosis**

It is the condition where diffuse epidermal hyperplasia leads to thickening of the skin. It implies increased thickness of the combined layers of stratum basale and stratum spinosum.

## **1.3. MESENCHYMAL HISTOLOGY MARKERS:**

For the mesenchyme that underlies the epithelium that forms the stroma and is a target tissue of malignant cell behavior with invasion, the histology markers are:

### **1.3.1. Blood Vessels**

Blood vessels develop multiple abnormalities as a result of the cancerous environment of tumor growth. Conventional hierarchy where arterioles connect to capillaries which in turn connect to venules that are absent in tumors.(Christopher and Mary 2001) Endothelial cells don't form a tight barrier and pericytes are loosely attached which is

associated with leakage from vessel structures. The vascular basement membrane created as a result of digressing and regression of vessels provides a marker for the dynamic nature of the tumor vessel.

Blood vessels are naturally proliferating, remodeling and lack regular shapes and normal hierarchical arrangement of arterioles, capillaries and venules. Tumor growth is dependent on angiogenesis and these components such as endothelial cells, mural cells and basement membrane display abnormal behavior. These severity and types of vascular defects within the tumor growth can be used as a histological marker to predict tumor growth.(Alonso and Fuchs 2003) Normal vasculature shows hierarchy of arterioles, capillaries and venules accompanied by pericytes. Structurally, pericytes are known to be associated with endothelial cells and within the basement membrane. Defects in the epithelial basement membrane depict well documented features of invasion when compared to the vascular basement membrane. (Gregory and McGarry Houghton 2011)

Untreated tumor has disorganized network of vessels that lack conventional hierarchy. Endothelial cells of tumors lack tight endothelial monolayer which is essential for normal barrier functions. Gaps between endothelial cells, irregularly shaped pericytes found in between the endothelial cells and basement membrane show multiple layers. Many vessels that are regressed produce empty sleeves of basement membrane whereas the normal vessel shows a cylindrical shape. Loss of endothelial cells does not correspond to loss of pericytes as some can be observed surrounded by basement membranes but not accompanied by endothelial cells.(Gregory and McGarry Houghton 2011)

The features described above as are variable in physical continuity but with tissue sectioning presentation is also likely to be effected and increase variability. For these reasons we do not focus upon this characteristic in our pattern recognition study during oral carcinogenesis.

### **1.3.2. Stromal Cells:**

A functional link exists between OSCC growth and the number of inflammatory cells present in the tissue and this is the premise for us to use inflammatory infiltration (II) in our analysis to improve fractal dimension (FD) analysis.

The inflammatory infiltrate is composed of granulocytes (eosinophils, basophiles, and polymorphonuclear leucocytes), NK cells, and mast cells to form the innate immune compartment and macrophages /dendritic cells, and lymphocytes (T and B populations) which are components of adaptive/acquired immunity. These cells are the major immune effector cells that contribute to development of premalignant and malignant tumors. There are also a vast number of cytokines, lymphokines, interleukins, chemokines, growth factors, immune modifiers and toll like receptors that effect epithelial cell growth and response to changes in micro or macroenvironments ( Piva MR, DE Souza LB, Martins-Filho PR, Nonaka CF, DE Santana Santos T, DE Souza Andrade ES, Piva D. Role of inflammation in oral carcinogenesis (Part II): CD8, FOXP3, TNF- $\alpha$ , TGF- $\beta$  and NF- $\kappa$ B expression. Oncol Lett. 2013 Jun; 5(6):1909-1914. Epub 2013 Apr 11)

## **Mesenchymal Cell Types**

Fibroblasts control the remodeling of ECM thus affecting proliferation, morphology and survival of the cells. Neoplastic programming of these stromal tissues is carried out by the inflammatory along with the active participation of the fibroblasts.(Reibel 2003)

Stromal cells respond to tumor growth by disorganized epithelium and dense fibrous interlobular tissue growth. In neoplastic tissue development, vessel densities and branching increase along with stromal vascular structures dilation is observed. (Hasebe, Konishi et al. 2005). In case of ductal carcinoma, stromal infiltration of inflammatory cells in dense collagenous stroma becomes very evident but less recognizable in OSCC.(Alonso and Fuchs 2003).

## **1.4. HISTOLOGY CHANGES IN PRE-MALIGNANT & MALIGNANT DIAGNOSIS**

Distinct tissue alterations are associated with premalignant and malignant change. Some of the cells display inappropriate and immature differentiation with a slight difference from normal cells and this is termed by the pathologists as atypia. Dysplasia can also be described in terms of differentiation and anaplasia which corresponds to a degree of disorderly changes from non neoplasia to a more pronounced appearance with neoplasia.(Krishnan, Venkatraghavan et al. 2012).

In general, premalignant dysplasia and malignant OSCC depicts a loss in uniformity of individual cells and architectural orientation. In the methods and results sections we describe in detail our assessment of dysplasia. For example, dysplastic tissues show hyperkeratosis, hyperplasia, anaplasia, and acanthosis. Specific cells are expected to show with varying degrees of pleomorphism, hyperchromatism, increased mitotic

activity, bizarre mitoses, nuclear-cytoplasm ratio reversal, chromatin clumping, karyorrhexis, pyknotic nuclei, and dyskeratosis.

Animal models for oral carcinogenesis demonstrate this identical set of pre-malignant & malignant tissue and cell changes but the presentation in terms of quantity and quality (degree) can be different. These differences are dependent upon the carcinogen inducer. For this reason it is important to use a carcinogen type and concentration that mimics human exposure experience. In this way we reduce another possible variable that would decrease association between the animal model and human exposure experience.

Another common feature noted to occur to stem cell and stem cell like progenitor populations that are contributing to clonal expansion and oral carcinogenesis is dedifferentiation. This feature describes histological change for the appearance of a primitive form of cell and nuclei. (Cheon and Orsulic 2011). These keratinocytes display abnormal cellular densities. The basal cells display nuclear hyperplasia (enlarged nuclei), dark stained nuclei (hyperchromatism), enlarged eosinophilic nuclei and higher reversed nuclear-to-cytoplasmic ratio. (Warnakulasuriya 2001). Features such as increase in mitotic activity, formation of enlarged mitotic features or presence of activity in unusual locations can be perceived with abnormal bizarre mitosis.

Another key alteration observed in epithelial dysplasia is a condition called dyskeratosis which corresponds to premature production of keratin in basal and supra basal cells. This inappropriate differentiation is an attempt to recapitulate keratosis observed in the stratum corium, surface layer.

Keratosis in the form of dyskeratosis is also noted in “keratin pearls” and these sites are represented by tight concentric rings of flattened keratinocytes that appear as well differentiated OSCC invade deeply into adjoining stroma tissue (Speight, Farthing et al. 1996)

### **Use of Histopathology Markers**

The tissue morphological changes like hyperkeratosis, basal cell hyperplasia, and acanthosis are common histological markers to predict changes in the tissues and to grade dysplasia. Epithelial rete peg processes with bulbous enlargements called drop-shaped rete peg processes are also important premalignant tissue changes. These are usually seen with secondary projections or nodules at the basal layer which further branch at indifferent angles into the lamina propria and connective tissue papillae. Severe epithelium dysplasia and carcinoma display loss of stratification and rete peg growth becomes disorganized as they display immature differentiation from basal cells to prickle cells to flattened keratinocytes.

### **1.5. GRADING & EVALUATION OF HISTOPATHOLOGICAL TISSUES:**

To grade a histopathology section requires an assessment of histopathology changes noted above. The higher the grade the more differentiated the mucosa is described which means it appears more normal and the specific site from which the tissue section was harvested can be recognized.

Oral tissues have variable clinical appearance so they are graded based on the combination of tissue and cellular damage. A variable histopathology appearance is a product of a heterogeneous exposure to etiology factors. For this reason we use

experimental animal tumor models to assess a specific tissue and cell relationship with limited confounders as found for human derived tissues.

Different pathologists place emphasis on different aspects of alterations thus arriving at various different diagnostic conclusions. This is due to variability discussed above, and the lack of a distinct entity and absence of accurate clinical markers to identify them. (Gupta, Mehta et al. 1980)

The World health Organization defines the morphologically altered tissues or generalized cellular states in which the tissues are more likely to become malignant. The features of cellular and tissue changes found in the tissues are characterized by variations in cellular proliferation and maturation of the squamous epithelium. They often manifest in the form of irregular stratification and increased keratinization of cells. (Pindborg, Reibel et al. 1985)

Histological changes contribute to diagnosis of epithelial dysplasia as described above (Warnakulasuriya 2001). A list of cell characteristics that are noted during histopathology assessment include: Loss of polarity of the basal cells, which is a loss in normal orientation of the basal cell populations to form a palisading or squamoid front with a well-defined basement membrane. The presence of more than one layer having a basaloid appearance is associated with an inappropriate extension of basal type cells to supra-basal, stratum spinosum layers. Often basaloid appearance is accompanied by dyskeratosis and other features noted above that contribute to a loss of differentiation. Drop-shaped rete-ridge, noted above is a feature that usually indicates an abnormal growth of rete-peg structures. This feature when accompanied with additional cell

abnormal histopathology characteristics noted above also identifies a rapid growth spurt into the underlying mesenchyme. Increased nuclear-cytoplasmic ratio reversal was discussed above and is an important identifier for moderate to severe dysplasia and OSCC. Nuclear hyperchromatism is an early marker for premalignant and malignant development. Hyperchromatism occurs as an alteration from euchromatin is changed to heterochromatin with associated clumping throughout the nucleus. Enlarged nucleoli can be associated with a variety of processes that affect hemodynamics flow, presence of inflammatory factors, infection derived virulence, and susceptibility related to DNA repair. Enlargement is derived from a change in surface volume and osmotic-oncotic pressure across nuclear membrane. Increased number of mitotic figures and bizarre mitotic figures demonstrate the physical organization of cells to proliferate with regulation or loss of this control. Aggressive growth behavior of keratinocytes is ascribed to increased numbers of a cell population with increased numbers of cells showing loss of mitotic activity. The presence of mitotic figures in the superficial half of the epithelium is a hallmark of an extension to this general lack of regulation of growth.

### **Disorderly maturation seen in epithelial dysplasia**

We have described above many features ascribed to loss of cell and tissue organization. Some of the more important characteristics are cellular and nuclear pleomorphism; irregular epithelial stratification; loss of intercellular adherence; keratinization of single cells or cell groups in the prickle cell layer

When biopsies from lesions are subjected to microscopic examinations, pathologist's grade is based on the microscopic features mentioned above. The more prominent and more numerous these features, the more severe is the dysplasia.



Most pathologist grades are in disagreement when it comes to mild and moderate oral dysplasia and severe dysplasia, carcinoma-in-situ and OSCC. This is because there is no standard that is available to supply a rigorous guideline for tissues that come from a variety of etiologies and presentations. To overcome this disadvantage, patterns for change are needed to attach a systematic organization to assist with a grade. To begin this process we are presenting in our study use of a fractal dimension analysis with enhancement with previously identified histopathology criteria that have clinical prognostic value.

Histopathology changes can be gleamed from the Brandwein histopathology criteria system.

#### **1.5.1. Brandwein histological model for predicting tumor development:**

These criteria set use variables that include: pattern of invasion, degree of keratinization, lymphatic response and mitotic rate. For human tissue histopathology analysis these features are used to determine the stage of cancer development. Patten of tumor invasion can be defined as the manner in which the cancer infiltrates the tissue at the epithelial-mesenchymal or tumor/host interface.

Neoplasia infiltrating in a widely dispersed manner are more aggressive than those growing in a bulky pushing model and this general characteristic is observed and designated as patterns of invasion (POI).(Brandwein-Gensler, Teixeira et al. 2005). This approach along with other variables serves as a rationale decision maker for pathology at the tumor site.

### **Pattern of invasion at the host/tumor interface:**

**POI Type 1:** Tumor invasion in a broad pushing manner

**POI Type 2:** Tumor invasion with a broad pushing finger or separate large tumor islands, with a stellate appearance

**POI Type 3:** Invasive islands of tumor greater than 15 cells per island

**POI Type 4:** Invasive tumor islands smaller than 15 cells per island including single cell invasion. This includes strands of tumor cells in a single-cell filling pattern, regardless of island size.

**POI Type 5:** Tumor satellites of any size with 1 mm or greater distance of intervening normal tissue at the tumor/host interface.

Further two more variables were created to take aggressive invasion into account. Predominant POI (PPOI) and worst POI (WPOI) were determined by measuring the POI at the tumor interface.

**Lymphoid infiltrate** at the tumor/host interface was quantified.

**Pattern 1:** Continuous and dense rim of lymphoid tissue at the interface

**Pattern 2:** Patches of dense lymphoid infiltrate with discontinuous inflammation along the interface.

**Pattern 3:** Patterns without lymphoid patches and lymphoid response.

Perineural invasion was defined as carcinoma specifically tracking along or within a nerve. It was further classified as involving large nerves (diameter > 1 mm) or small nerves (diameter <1mm).

Pathological grade was designated for other variables such as

Keratinization can be quantified as >50%, <50% and <10%; nuclear grade: well, intermediate, and poor);

Foreign body reaction: 1 or higher power field, none.

Eosinophilia, lymphatic or vascular tumor emboli and carcinoma in situ in mucosal adjacent to tumor are graded based on their presence in the particular tissue slide.

### **Margin Analysis:**

Group 1: Greater than or equal to the 5 mm clearance at initial resection

Group2: Inadequate margins during intra-operative consultation, final margin greater than or equal to 5mm after harvesting supplemental margins.

Group3: Final permanent pathology revealing close (<5mm) margins

Group4: final permanent pathology revealing frankly positive margins.

In our study we have used Brandwein criteria as a starting point for evaluation of experimental Syrian hamster tumor tissue because this tissue does not have all the features noted above for human tissue sections.

Our scoring was based on pattern of invasion and inflammatory infiltration but we did not include perineural infiltration because a lack of this feature in hamster tissues.

Risk classification algorithms were generated by Brandwein to classify patients as low, intermediate and high risk. Each variable were assigned point assignments for the particular features which led the model to discriminate from intermediate to high risk conditions correlating with local recurrence and overall survival. (Brandwein-Gensler, Smith et al. 2010). This assessment was supplanted in our study with fractal dimension analysis.

### **1.5.2. Diagnostic assessments of Dysplasia**

In order to assess the various stages of cancer development, it is important to understand the basic terminologies. This helps us understand the underlying principle to this study.

**Atypia:** This pathological term is defined as the condition with a structural abnormality in a cell which describes the precancerous indications associated with later malignancy.

**Dysplasia:** This pathological condition refers to an abnormal development consisting of expansion of immature cells with corresponding decrease in the number and location of mature cells. Dysplasia can be graded according to a combination of cellular and tissue change subjectively in to less severe and very severe tissues. Oral epithelial is subdivided into mild, moderate and severe conditions. The grading of dysplastic oral epithelium takes the degree of cellular atypia and altered lesions into consideration. (Tabor, Braakhuis et al. 2003)

**Mild Dysplasia (Grade I):** this condition involves the proliferation of the immature basal cells above the para-basal region up to two thirds of epithelium.

**Moderate Dysplasia (Grade II):** Proliferation in the middle of the epithelial cross section can be observed.

**Severe Dysplasia (Grade III):** can be observed with abnormal proliferation from the basal layer to the upper part of the epithelium.

## **1.6. ENVIRONMENTAL FACTORS AFFECTING OSCC**

### **1.6.1. Age**

Increase in age is often an indicator for risk for OSCC. There is also an indication for enhanced incidence among young women for OSCC. Oral cancer is often a disease of

older age, and about 95% of oral cancer is observed in persons over 40 years of age. This time factor operates in conjunction with predetermined changes in the biochemical and biophysical processes such as nuclear, enzymatic, metabolic and immunologic processes of aging epithelial cells. These changes are influenced by exposure to chemicals (e.g., toxins, mutagens, and carcinogens), viruses (e.g., human papilloma virus, and possibly herpes viruses), hormones (e.g., parathyroid, thyroid, and estrogen), nutrients (e.g., proteins, lipids, carbohydrates, vitamins or minerals) or physical irritants (e.g., dental appliances, oral habits). Thus the rate of turnover of keratinocytes for different oral mucosa sites is slightly different. For example, the more keratinized the mucosa surface, the slower the turn-over rate which averages 21 days. A result of the turnover rate is a modification of apoptosis (programmed cell death). Apoptosis can be modified by factors that alter growth factors and suppressor proteins such as Bcl-2 (B cell lymphoma derived factor 2) which affects cytochrome c release from the mitochondrion to affect cysteine proteases that include caspases (e.g., procaspase and activated caspase 3 ). This effect is notable because it is a persistent characteristic found in malignant transformed keratinocytes. [Zakeri Z].

The impact of age can be further observed by the fact oral cancers occur often in persons over 65 years of age with a demonstration of immunosuppression in both innate and adaptive compartments. Among younger persons under 40 years of age, environmental factors such as use of smoking products (e.g., tobacco products and marijuana use) oral sexual exposure, with poor oral hygiene in association with immunosuppression are recognized associations linked to development of OSCC.

### **1.6.2. Ethnicity**

Ancestry also appears to affect the risk for OSCC. Among individuals of African ancestry initial presentation of OSCC shows aggressive and local and distant growth. Reason for this type of aggressive growth behavior is not clearly delineated. Some studies indicate that this biologic effect may be a consequence of lack of access to medical care. Others suggest presence of susceptibility gene expressions that are expected to increase metabolism of known etiologies such as ethyl alcohol and polycyclic aromatic hydrocarbons (PAH) and nitrosamines. However, there are large numbers of individuals from other ancestries that also present with aggressive OSCC which seem to indicate that presentation of aggressive growth of OSCC is linked to exposure experience and timing of medical diagnosis (Li. R (2013)).

In term of relative numbers in the United States oral and oro-pharyngeal cancers are the fourth leading cancer in black men and the seventh leading in non-Hispanic white men. Oral carcinogenesis occurs less frequently in Asians and Hispanics than the other races but this pattern changes world-wide.

Even if there are proof for the genetic factors, the difference in habits and lifestyle play an important role. As the genetic code is unraveled, inherited risks are further clarified.

### **1.6.3. Habits**

#### **Tobacco**

Epidemiology studies have shown that use of tobacco increases risk about two fold for OSCC. Benzo[a]pyrene a tobacco derived PAH binds to nucleoproteins and creates DNA bulky adduct particularly at cytosine-guanosine islands of CpG which create mutations specific on nucleotides promoter sites that regulate tumor suppressor gene

activities such as for p53 and Rb ( Wang H.T. (2012)). Tobacco use includes cigarettes, cigars, pipes and smokeless preparations. (Singh 2008). Nitrosamines and derivatives; such as, acrolein, the most potent tobacco specific nitrosamine (TSNA) are released by metabolism of nicotine after generating tobacco smoke or placement of smokeless products in the mouth(Mognetti, Di Carlo et al. 2006).

In this study we evaluate the PAH, tobacco derived carcinogen DBP to demonstrate that this carcinogen is highly potent and can produce at low dose (0.0025 mM/ 2.5 nM/application)an OSCC in every animal exposed for 25 weeks (3X/wk).

## **Alcohol**

Observations in many populations have shown ethyl alcohol use is a major etiology for development of OSCC and other cancers of the gastrointestinal tract including upper and lower regions (Haas SL (2007)).

Specifically the metabolism of ethyl alcohol through the expression of polymorphic variants of genes for alcohol dehydrogenase, aldehyde dehydrogenase and retinoid dehydrogenase results in synthesis of acetaldehyde which is a DNA damaging agent and carcinogen (Seitz HK, (2009)).

It has been observed that the ethanol can increase the incidence of tumors induced by N-nitrosodiethylamine, N-nitrosodipropylamine and vinyl chlorides. With this, acetaldehyde, enhances experimental benzo(a)pyrene tumors.(McCullough and Farah 2008).

Alcohol also has the tendency to act as a solvent which enhances the penetration of other carcinogens in target tissues which are topically exposed on tongue, floor of the mouth hard palate, and gingiva. Depending on the status of the liver and robustness of

DNA repair individuals can inhibit or detoxify carcinogenic compounds derived from alcohol consumption. One method induced through chronic alcohol intake is activation of enzymes of the cytochrome P<sub>450</sub> system and glucuronidation system which also activates the xenobiotic responsive elements and system in a variety of cells such as keratinocytes. (Dorne JL (2005))

It is well recognized that the oral cavity contains about  $2 \times 10^{10}$  microbes with about 600-800 different taxa. Many of these microorganisms can metabolize alcohol to release acetaldehyde and in this manner assist during induction of oral carcinogenesis (Schwartz. J (2011))

### **Loss of Dentition/ Dental hygiene**

Epidemiology studies have confirmed a significant association between the losses of dentition caused by oral infection and increased risk for OSCC. (Marshall. JR (1992)).

For example, neoplastic growth can be observed in areas of prosthetic appliances which may develop as a result of a cause-and-effect relationship. Studies have also shown a co relation between chronic dental irritation and OSCC because people with poor oral hygiene often have jagged teeth or fillings may irritate; induce inflammatory activities and create a wound which stimulates inappropriate repair.(Tosti A, Piraccini BM, Peluso AM. 1997 Dec; 16(4):314-9).

### **1.6.4. IMMUNOSUPPRESSION**

Immunologic surveillance which removes abnormally growing daughter cells produced by damaged clones of keratinocytes is a constant feature in oral mucosa. Immune activity for surveillance includes both innate and adaptive immune activities. These



activities therefore include the numerous immune effectors, and factors previously discussed above and later noted as composing an important infiltration to form a regulatory feature observed in both experimental oral carcinogenesis and in sporadic human OSCC tissue sections.

We also note the presence of the inflammatory infiltration is not a positive sign for inhibition of OSCC. We reason the inflammatory infiltrate that appears to grow in parallel with oral carcinogenesis contributes to a selection of DNA damaged keratinocytes as mentioned above. Moreover cells because of a poor or immature differentiation state evade immune recognition and this permits their persistence in a proliferation pool of poorly growth regulated keratinocytes. Immune cell populations and keratinocyte cells will eventual coalesce to form OSCC. Each OSCC we further reason will have a pattern of growth at the tumor border which we recognize as a fractal dimension pattern which is linked to presence of immune cell infiltration.

Furthermore, immune competence and immune cell surveillance usually demises with age and simultaneously increases the risk of malignancy which is considered a reason for the incidence of OSCC rising with age. (Mognetti, Di Carlo et al. 2006)

## **1.7. IDENTIFICATION USING IMMUNOHISTOCHEMISTRY**

### **1.7.1. Standard Approach**

The basic concept of Immunohistochemistry is the demonstration of antigens (Ag) within the tissue sections by means of specific antibodies (Abs).(Rahman and Leong 1991) Once the binding occurs, a histochemical reaction is visible by light microscopy or flourochromes with ultraviolet light. The methodology of Immunohistochemistry becomes more complex as the requirement of sensitivity and specificity

increases.(Hofman 2001). This technique is commonly used in the diagnosis of abnormal cells found in malignant tumor. It is a valuable tool for both diagnosis and research of neoplastic diseases.(Yeh and Mies 2008).

### **1.7.2. Protein Interactions of Immunohistochemistry**

From a biochemical point of view, the antigen-antibody bonds are weak hydrophobic and electrostatic interactions. The commonly observed interactions are the inter-atomic or inter molecular hydrophobic bonds, Van der Waals forces and Hydrogen bonding.(Hofman 2001) Antigen-Antibody complex formed can be expressed in terms of affinity constant. The range varies from below  $10^5$  litre/mol to  $10^{12}$  liters/mol. Higher affinity Abs will bind to more Ag in shorter incubation time thus leading to more diluted antibody solution.

**Polyclonal Antibodies:** They are produced in multiple animal species. They have higher affinity and wider reactivity but lower specificity compared to monoclonal antibodies. These antibodies have the advantage of identifying multiple isoforms. They can also pose a disadvantage because they have a high likelihood of cross-reactivity with similar epitopes in other proteins. (Cregger, Berger et al. 2006)

**Monoclonal antibodies** are generally produced in mice by injecting a purified immunogen thus producing an immune response. The B-lymphocytes are harvested in the spleen and fused into mouse myeloma. This is followed by selecting hybridomas (hybrid cell) of desired specificity. A hybridoma can be defined as an immortal cell which can produce antibodies for a single epitope. They are highly specific when compared to polyclonal antibodies. (Cregger, Berger et al. 2006)

### **1.7.3. Fixation**

Fixation of tissues is necessary to preserve the cellular soluble and structural components of the cell. It prevents autolysis and displacement of cell constituents against deleterious effects. Two major types of fixation of tissues carried out in histopathology are using cross-linking fixatives and coagulating fixation. Commonly formaldehyde is the gold standard of fixatives for routine histology and immunohistochemistry. Formalin fixation is a progressive, time and temperature dependent process. The Antigens can be retrieved using protease enzymes which digest the proteins to get the antibodies back to their original form. (Hofman 2001)

### **1.7.4. Types of IHC Methods:**

Popular IHC detection methods are based on either chromogenic or flourogenic based process mediated by an enzyme or fluorophore respectively. With chromogenic reporters, the enzyme label reacts with the substrate to produce an intense colored product which can be observed under a light microscope. Alkaline phosphatase and horseradish peroxidase is the most commonly used enzymes as labels for protein detection. Depending on the sensitivity of the immune reaction, different detection systems can be used. They are majorly classified as either direct or indirect detection methods.

#### **1.7.5. Method of Staining using IHC methods:**

Direct method is a one step process with primary antibody conjugated with a reporter molecule such as fluorochromes, enzymes or biotin. This method is simple but lacks sensitivity for the detection of most antigens. To overcome this, the indirect method of detection was developed where the first layer of antibody is unlabelled, but the second layer raised against the primary antibody is labeled. As the primary antibody is not labeled, it can retain its activity resulting in a strong signal, and the number of labels per molecule of antibody is high thus increasing the reaction signal. Some of the commonly used indirect methods are Avidin-biotin method, Peroxidase – antiperoxidase (PAP) methods, polymeric labeling two-step methods, tyramine amplification methods and immune-rolling circle amplification methods.

#### **1.7.6. Advantages of IHC methods:**

Most common advantages of immunohistochemistry technique are that they are routinely available and relatively inexpensive. They are automated systems which are rapid and can connect visualized target with microscopes. This method helps study the antigens, the protein levels and activities; that differ from those of RNA. Even with these advantages, the method involves complex standardization techniques and difficult antigen retrieval & quantitative techniques. This requires well trained pathologists and lab personnel for standardization and interpretation of the results.

#### **1.7.7. Immunohistochemistry (IHC) in cancer:**

Tumor markers are signals or representatives from the cancerous malignant cells which are commonly enzymes, oncogenes, tumor-specific antigens, tumor suppressor genes

and tumor proliferation markers. More than 20 tumor markers have been developed for clinical use. Immunohistochemistry is a technique which helps in visualizing these tumor markers to effectively predict oncogenesis, diagnose a cancer as benign or malignant, and determine the stage and the grade of cancer.(Rahman and Leong 1991)

## **1.8. FRACTAL DIMENSIONS**

### **1.8.1. History**

Fractal analysis is the contemporary method of applying non-traditional mathematics to measure complexity of patterns that defy understanding with the Euclidean concepts. Fractals can be observed in nature such as meandering coastlines, growing crystals and swirling galaxies. Theoretically fractals are abstractions, but the subject of fractal analysis such as digital images limited by screen resolutions, are not true fractals in the real sense.(Karperien 1999). Similarly, the fractals found in nature are not infinitely scaled, thus like computer generated patterns, are generally only approximations to the fractals in the strictest sense. Fractals are defined as having an irregularity that prevents them from being defined by the Euclidean geometry, and especially of being self similar- that is, being composed in such a way that the shape can be split into part, each of which is approximately a reduced –size copy of the whole. (Mandelbrot 1977)

### **1.8.2. Fractal geometry**

The Euclidian geometry has many deficiencies when applied to biological systems. A pure mathematical fractal object .i.e. a Julia set (Cross 1997). The Julia set has

complex boundaries and this level of complexity remains constant as the magnification increases. Histopathologists recognize this similarity when they observe carcinogenic tissues under the light microscope. The complexity of the tumor remains same, where the smooth cell membrane is the constant feature so the absolute measurement of the parameters such as perimeters is not possible. Mandelbrot thus plotted the measured parameter at different magnifications on a log-log graph, which gives a straight line taking the gradient of the line as the fractal dimension. Fractal dimension is thus the index of the space-filling properties of an object such that the closer the dimension is to the topological dimension in which the object is embedded, greater is its space filling properties.(Mandelbrot 1977) The fractal dimension also leads to the definition of a fractal object, which is an object whose fractal dimension is greater than its topological dimension. For biological objects the fractal dimensions require to be empirically measuring and statistically comparing with topological dimensions.(Karperien 1999)

Most commonly used tools in cancer are box-counting dimension, pixel dilation method and the perimeter stepping (or divider) dimension. This involves an image to be digitized and converted to a single pixel outline by an appropriate algorithm. Boxes of varying sizes are applied to the outline, and the number of outlining squares is counted. Formula for the box counting squares is given by

$$D_B = \text{the slope of } (\ln N / \ln \varepsilon)$$

This equation determines how number of parts  $N$  changes with scale  $\varepsilon$  ([box size/image size]) where  $D_B$  is the box counting dimension.

### **1.8.3. ImageJ & Frac-Lac Plug-in**

ImageJ is a public domain, Java-based image processing program developed at the National Institute of Health. It was designed with an open architecture that provides extensibilities via Java plugins and recordable macros. Custom acquisition, analysis and processing plugins can be developed using ImageJ's built-in editor and Java compiler. It supports image stacks (series of images that share a single window), and it is multithread, so time consuming operations are performed parallel on multi-CPU hardware. User written plugins help solve many image processing and analysis problems from 3D Live processing to radiological image processing.

Frac Lac is a plugin used for objectively analyzing complexity and heterogeneity of binary digital images. It measures difficult to describe geometrical forms where the details of design are as important as gross morphology. This is very useful to measure branching structures and textures of biological cells and structures. This plug-in mainly performs different types of analysis to deliver data and graphics for fractal dimension, lacunarity, multifractal data, size and shape of patterns in binary images (Karperien 1999). Regular box counting, subscans, sliding box lacunarity and multi fractal scans can be done on FracLac.

### **1.8.4. Fractal geometry and Cancer**

Fractal geometry which consists of a vocabulary of irregular shapes describes the pathological architecture of tumor, their growth and angiogenesis. Cancer can be characterized by irregular shapes, poorly regulated growth which usually doesn't follow the rules of traditional Euclidean geometry. The cancerous cells, tumors and

vasculature can be explained in detail by fractal geometry by focusing on irregularity of tumor growth rather than on a single measure of size. (Baish and Jain 2000). The irregular boundaries of tumors can be analyzed by fractal geometric analysis and many tumors have shown to have fractal dimensions larger than their topological dimensions. Malignant melanomas can be distinctively discriminated from the benign ones. Some studies have used fractal analysis to study the nuclear dimensions and texture for the prediction of prognosis for prostatic cancer.(de Arruda, Gatti et al. 2013) The fractal texture of the nuclear chromatin patterns have been a useful discriminate function in differentiating the nuclei of benign and malignant cells. Dysplastic and malignant epithelial lesions in the oral cavity have been observed and studied using fractal tools such as box counting and perimeter stepping methods to measure the fractal dimensions of the epithelial- stromal interfaces in the lesions. Along with these methods, local fractal dimensions are measured which give a distribution of frequencies of the fractal dimensions across the whole lesion.(Kaye 2008) They are mainly based on irregularities of many sizes which are explained by examining how the features of one size is related to number of similarly shaped features of other sizes. We try to apply approximate fractals to cancer for determining the morphology of the tissues which further can be developed for diagnostic and prognostic purposes.

Standard for confirmative diagnosis is carried out mainly based on qualitative histopathological evaluations backed by clinic-pathology acumen of medical experts.(Krishnan, Venkatraghavan et al. 2012) Visual examinations, of radiological images, biopsy specimens and tissues are qualitatively interpreted based on their abnormal structural irregularities or high cell growth. Fractal geometry intends to



develop a more quantitative and a higher reproducible method to analyze these images. Computational tools with fractal analysis approach use the measure of irregular structures to quantify tumor growth.

Ultimately, the real value of this measurement is that it provides an objective, quantitative approach for classifying organization which is difficult for the pathologists to do by the eye. Some available software such as ImageJ's Fractal dimension and Lacunarity plug-in can quantitatively assess the images for this measurement with some user interaction and troubleshooting(Kam, Karperien et al. 2009).

## **1.9. ORAL CARCINOGENESIS ANIMAL MODELS**

### **1.9.1. Need For Models:**

Investigation of the progression of the disease and elaboration of diagnostic or therapeutic protocols require animal models. They have to be biologically and clinically relevant to the diagnostic process. These models help understand the molecular mechanisms involved in the initiation and progression of the tumor, explains the development of malignancy in oral cancer thus improving the prognosis and elaboration of new treatments.(Mognetti, Di Carlo et al. 2006)

### **1.9.2. Advantages of Animal Models:**

Animal models can represent cellular and molecular changes associated with the initiation and progression of human cancers and are thus of crucial importance. This has been of particular importance especially with chemically induced oral cancer.(Cheon and Orsulic 2011) Animal models help analyze the development of

cancer, emphasizing pathogenesis of neoplasia, with integration between the cellular and tissue biologic levels, thus offering major opportunities to generate important new insights onto the nature and genesis of neoplasia. (Gimenez-Conti and Slaga 1993).

### **1.9.3. Disadvantages:**

Rodent models have different metabolism, turnover rates for cells, physiology responses to toxins, mutagens and carcinogens compared to human tissues and cells. For example, many chemicals that are toxins, mutagens and carcinogens in rodents are not found to have these activities in humans. It appears there is a greater capacity for DNA repair and protection from carcinogenesis in human tissues compared to rodent tissues. In addition the activity of a toxin, mutagen or carcinogen in rodent models is compressed and this also effects some physiology and biochemistry activities..(Gimenez-Conti and Slaga 1993).

### **1.9.4. Hamster Model in OSCC**

Syrian hamster cheek pouch has been widely used because of its anatomical and physiological features. One pouch under the cheek muscle opens into the anterior part of the oral cavity, which is further associated with small salivary glands producing serous and mucous secretions.(Gimenez-Conti and Slaga 1993) The buccal cavity is lined with keratinizing squamous epithelium. Chemical carcinogenesis induction is most extensively studied in the Hamster cheek pouch model.

#### Advantages of Hamster model:

Studies based on hamster buccal pouch model have provided an array of changes that are analogous to those observed in human invasive oral carcinoma. The expression is observed in malignant tumors of the pouch and early stages of tumor development, but not in normal oral mucosa. The technique for carcinoma induction is simple and does not require any anesthesia. Evaluation of cancer development can recapitulate histopathology methods used for human oral tissues. The surface area of the pouch is relatively large which allows easy accessibility to view the change in mucosa. (Shklar and Schwartz 1993). The “initiation and promotion” multistage tumor development in the hamster buccal pouch model allows the correlation of genetic changes with the histopathological changes of dysplasia through carcinoma to invasive squamous carcinoma. (Reiskin and Berry 1968) The hamster has several areas of uniqueness which must be considered in evaluation of results from oral carcinogenesis studies. (Gimenez-Conti and Slaga 1993)

The hamster model reflects many aspects of human oral cancer development. They display common features, biochemical and molecular similarities to human cancers such as change in oncogenic expression such as p53 and or the ras proto-oncogene, tumor necrosis factors, transpeptidase, increase in low molecular weight keratins, immune derived cytokines and enhancement of growth in response to various factors.

#### Disadvantages of Hamster model:

The Syrian hamster population has been derived from a small breeding pair resulting in restricted polymorphism. In addition to this the number of T-cells in the hamster spleen

exhibits a lower number/gram weight of the organ when compared to a mouse or human.

Hamster's intraoral tissue is histologically different from human oral mucosa; it is considerably thinner and has a single submucosal connective tissue and the human mouth is devoid of a pouch similar to that of the hamster. For this reason it is important to focus upon oral tissues such as tongue and floor of mouth.

There is a reduced antigenic recognition and cytotoxic T-cell responses which is enhanced by a delay in vascular drainage and lack of lymphatics in the buccal pouch (Giunta, Schwartz et al. 1985).

#### **1.9.5. Rat/Mouse Model in Oral Carcinogenesis:**

As an alternative to hamster for oral carcinogenic models, are rat/mice models. A multistaging system was developed for the mouse model and subsequently tumor growth is promoted but often inappropriate carcinogens that humans are not exposed are used such as 7,12 dimethylbenz[a]anthracene (DMBA) and 4-nitroquinoline oxide (4NQO) (Cheon and Orsulic 2011). In addition other mouse models for OSCC induction used a endogenous murine mutation in p53 tumor suppressor gene or exogenous orthotropic creation to amplify mutation an effect not observed in human OSCC.( Acin S, Li Z, Mejia O (2011)).

An example of rat or murine oral carcinogenesis is a rat model exposed to fore-mentioned carcinogens induced tongue lesions in comparison to cancer of the palate in the mouse. In this rat model, increased levels of polyamine synthesis along with nucleolar organizing regions (NOR) along with progression of oral carcinogenesis was

observed.(Raju and Ibrahim 2011). Mouse model demonstrates some molecular mimicry of human oral cancers, similar to the hamster model. Increased expressions of EGF receptor, point mutations and LOH involving guanine- to-adenine transition at HA-ras 1 codon 12 on mouse chromosome 7 was noted (Mognetti, Di Carlo et al. 2006).

In C57Bl/6J mice and in CD-1 mice DBP application has been shown to produce oral premalignant dysplasia and OSCC but further studies are required to

#### **1.9.6. Animal model used in this study**

##### **Improvements over prior models:**

The model used in this study is a controlled carcinogenesis Golden Syrian Hamster tumor model that used the carcinogen, dibenz [a, l] pyrene (DBP) (0.0025 mM dissolved in acetone (1.0%, v/v) applied to the floor of the mouth and lateral border of the tongue (2.5 nM/ application). The control was acetone (1.0%, v/v) application applied to the identical tissue.

There is no effect of external environmental factors in the hamster model, thus adding precision. This model was used in a fractal dimension analysis that combined histopathology with an emphasis on pattern of growth, inflammation infiltration, and protein expression that represented cell distributed throughout the mucosa and specific basal cell populations. This is unique and we suggest provides a better understanding of the oral carcinogenesis process by examination of the tumor growth front as the primary region to attain information for increased accuracy of histopathology diagnosis.

## **1.10 CHEMICAL CARCINOGENESIS**

Carcinogenic process can be elucidated by understanding the chemical and physical properties of chemical carcinogens, their immediate interactions with the target and other tissues. Increasing study of the responses of living organisms and tissues to a wide variety of toxic agents at both biochemical and biological levels of organization has made it evident that they are subjected to similar types of agents and elicit similar change (Berenblum and Shubik 1947). Study of different processes constituting chemical carcinogenesis helps in developing a rational understanding of cancer induction and means to diagnosis at early stages.

Cancer development with chemicals begins with a brief exposure to an activated form of carcinogen, where it can act only as a stimulant and need not be present as such ever again. This brief exposure to the chemical induces a cell that can be differentially stimulated to produce a focal proliferation (Yuspa and Poirier 1988). A neoplastic cell is one that can proliferate without the need for a known stimulus for growth. i.e. A cell has acquired some degree of autonomy. This state can be termed as the 'initiated state' which cannot be detected, but can be identified only by subsequent focal proliferation. Initiated state is intricately bound by the subsequent appearance of discrete proliferation (Singh 2008).

The initiation-promotion stage can be justified by its dependence of each of its steps on the environment for their appearance. After the initial exposure of the carcinogen, the environment determines its further steps. After the first sequence, a new population is generated which is at a greater risk for the second event is developed. This new focal

change and amplification is self-generating and not environmentally affected. This second event is termed as 'neoplasia' and all events preceding this is called the 'preneoplasia' (Berenblum and Shubik 1947). Thus, initiation can only be defined as a subsequent event in response to exposure to a promoting or selecting environment which are largely permanent and reflect some changes in the DNA. For example, activation of carcinogens cannot be equated to DNA-adduct formation with initiation. Many carcinogens such as dibenz[a,l]pyrene, and B[a]P can be activated to form adducts without initiating cancer in the system, but when coupled with one round of cell proliferation, they develop to form cancer in the tissues. Common hypothesis for cell proliferation in initiation stage involves the DNA synthesis or replication which fixes damage in daughter strand and for the cell proliferation to be effective, it should occur within 1-3 days after administration of the carcinogen (Tanaka and Ishigamori 2011).

In tissues with continuous proliferation, the initiation of carcinogenesis with chemicals depends on metabolic patterns of activation and repair, providing initial cells are retained (Schwartz 2000). Whereas in non proliferating tissues, initiation can act as the rate limiting step for beginning the process of carcinogenesis. Cell necrosis induced by viruses, toxic agents, parasites followed by cell regeneration is an important determinant for initiation of cancer.

Some common properties of the initiated cells are observed. The appearance of enzyme excess or deficiencies and other biochemical changes are used to identify pre-neoplastic cells (Mognetti, Di Carlo et al. 2006). Another effect is the resistance towards inhibitory effects of carcinogenesis on cell proliferation. This effect can further be used to study the properties of initiation and initiated cells. Retention of a response

to mitogens by the initiated cells and the loss of response by the majority of surrounding cells on repeated stimulation is a functional property observed in initiated cells. This approach can be used as a model to study differential stimulation or promotion as well.(Reiskin and Berry 1968)

The term 'promotion' is analogous to the process of neoplastic development, tumor formation or cancer development. It is usually accelerated in a tissue that is exposed to an initiating dose or more doses of carcinogen. (Tanaka and Ishigamori 2011)

Model designed by Rous, Berenblum, and Mottram has laid the major foundation for the promotion of carcinogenesis. Biochemical, metabolic and biological effects are induced in normal cells using chemical carcinogens like phorbol esters which show similar effects which parallels effects in cells when exposed to single dose of a potent PAH . These effects include changes in morphology, microtubule proliferation, cell proliferation, enzyme induction, polyamine synthesis, phospholipid synthesis, membrane structures and functions, adenosine triphosphatases (ATPase), release of prostaglandins, inhibition and stimulation of differentiation in normal cells and cell lines. (1986).

In the model system presented here we used dibenz [a, l] pyrene (DBP) as both an initiator and promoter concentration dose. Either a reduction in time of exposure or concentration would provide an initiation of oral carcinogenesis with DBP. Promotion by DBP would subsequently have to be observed following a resting phase in which progenitor daughter basal cells that are non-viable because of DNA damage are eliminated from a proliferation pool. Remaining cells are expected to be DNA damaged,



exhibit abnormal growth, loss of apoptosis, demonstrate nuclear instability (e.g., epigenetic changes: methylation, acetylation, phosphorylation) and an increased risk for additional DNA damage which will cause formation of a malignant phenotype that will manifest by changes in tumor growth pattern and contribute to fractal dimension analysis.

### **1.11 CANCER STEM CELLS**

Cancer stem cells are newly identified subpopulations located in the basal stratum of the oral mucosa. These cells possess properties for differentiating into heterogeneous progenies of malignant cells. However, under normal differentiation states subject to maintaining normal oral mucosa architecture this characteristic is limited and restricted in oral keratinocyte, basal populations. During early development or malignant conditions of dedifferentiation oral epithelium can transform into mesenchymal type cells (e.g., carcino-sarcoma).

In regards to DNA environments, basal-progenitor keratinocyte populations are induced to undergo genetic mutations that lead to loss of tissue repair function but they retain some stem cell characteristics such as self renewal and plasticity to differentiate in tumor tissues.(Li, Heidt et al. 2007). These cells are resistant to biological or radiotherapeutic treatments and are suggested as responsible for tumor metastasis. Identifying carcinoma related stem cell-like populations would pave the way to understand development of cancer (Wang, Xie et al. 2012).

In our study we used the concept of cancer stem cells to add precision to identification of fractal dimension analysis through specifying cells with nuclear derived growth and

membrane changes linked to basal cell characteristics (e.g., PCNA and CD44). (Fujita, Sato et al. 2002).

## **2. METHODS**

### **2.1. Oral Carcinogenesis Model**

A study was conducted, with 25 Syrian hamsters (*Mesocricetus auratus*) (45 wks of age) for each of two groups. One was the control group which was administered through application (painting) of acetone (1%, v/v) using a #2 sable brush. The other group studied was administered dibenz [a, l] pyrene (DBP) (0.0025 mM/ 2.5 nM/application) dissolved in acetone (1%, v/v). Each animal in each group was treated three times a week for 25 weeks to the lateral border of the tongue (right side) and floor of the mouth.

### **2.2. Histopathology Assessment**

Evaluation of histopathology was based upon previously published criteria for human and hamster oral tissues (Schwartz 2000). Premalignant change was characterized as dysplasia and graded as mild, moderate, or severe.

- The features of dysplasia include hyperkeratosis, hyperplasia, and anaplasia. Additional characteristics associated with moderate dysplasia include: acanthosis, pleomorphism, increased nuclear cytoplasmic ratio reversal and mitoses. Severe dysplasia is further characterized with increased numbers of mitoses with some bizarre mitoses, and clonal expansion of basal keratinocytes into the underlying stroma forming a teardrop-shaped epithelial pattern.
- Oral squamous cell carcinoma has features that are an extensions of dysplasia listed above. Moreover, the pattern of invasion is associated with an extension of the abnormal severe dysplastic keratinocytes in deep stroma islands.

### **2.3. Determining Patterns of Invasion (POI)**

Histopathology classification by an experienced pathologist depends on a number of factors when any tissue sample is examined for example, where the biopsy tissue was harvested and the degree of similarity to any remaining tissue. As an aid, a guide to classifying histopathology based on pattern of tumor invasion (POI) has been constructed (Brandwein-Gensler, Teixeira et al. 2005). Although the guide was originally intended for use with human tissue, its categories translate well to analyzing oral hamster tissues given the controlled nature of the experiment, and parallel development of OSCC in the hamster tumor model. In addition, this hamster tumor model has more relevance and histopathology significance because induction of oral carcinogenesis was obtained following application of DBP an environmental carcinogen which humans are exposed.

POIs for this models included normal, premalignant-dysplasia and invasive OSCC.

**POI 1:** All histopathology POIs are quantified in comparison to normal broad, non-invasive front of normal mucosa cell growth.

**POI a, b, c:** Dysplasia was categorized into three separate categories to distinguish stages of severity and progression through tumor development: (a) Mild dysplasia, (b) moderate dysplasia and (c) severe dysplasia.

A general pattern of growth can be described for mild dysplasia: A small amount of invasive growth isolated to a single region of several cells, whereas moderate dysplasia shows a similar type of growth in multiple regions, often along a significant portion of the epithelial layer but not including all layers.

Severe dysplasia represents a finger-like pushing front, with a stellate appearance. It tends to represent more severe forms of dysplasia, hyperplasia, and atypia as described above and it may show early signs of OSCC development.

**OSCC; POI:** 2 for early and 3 for later incorporates more aggressive growth into surrounding tissues which is observed in dysplasia. In general these tissues display tumors that develop into islands (greater than 15 cells each) after breaking away from the original epithelial region and demonstrate a process of spread.

Euthanization of hamsters occurs shortly after development of cancer in order to reduce pain, as requested by the animal care committee, and this minimizes additional categories for severity that are associated with invasion into adjoining tissues to induce necrosis and atrophy.

Our POI guide was used to examine the epithelial layer and categorize the tissues according to a FD analysis. These diagnoses were then subjected to comparative assessment to evaluate significant change as described below.

#### **2.4. Tissue selection and Number**

We reviewed at least one tissue section from each animal composing the DBP group. We reviewed at least 5 separate areas at 20X magnification to evaluate for FD analysis in conjunction with POI.

For example, a total of 47 images were stained with stem cell marker, captured at 20X and analyzed using simple box count. The FracLac settings for box counting used boxes that ranged from a minimum of two pixels in size to a maximum size of 45% of the ROI.

## **2.5. Fractal Dimension Analysis**

In order to analyze the fractal dimension of the epithelial layer of each tissue sample, the slides needed to be converted to a digital format. This was accomplished using a Leica light photomicroscope equipped with a SPOT camera system. This microscope is equipped with objectives with magnifications of 10X, 20X, and 40X.

After converting to a digital format, the images were modified so that the epithelial layer would be the focus of the image. In order to do this, the RGB images needed to be converted using ImageJ, first to a greyscale format, and then to a binary image to reveal the edges of the epithelial layer (Rasband 2009). This process is shown visually in Figure 3 demonstrated in the Result section.

Converting from grayscale to binary required the user to properly threshold each image in such a way that the boundary epithelial layer would not be lost, while at the same time removing as much unnecessary information from the image as possible. With the threshold process completed, ImageJ could find the edges in the binary image, allowing the user to select the epithelial layer boundary as the region of interest (ROI) for the fractal calculation.

The basic algorithm for finding the FD of an image uses the following formula:

$$N \propto \varepsilon^{-D_F}$$

In an irregularly-shaped line whose FD is being calculated,  $N$  represents the number of pieces which the line can be broken into when using pieces of scale  $\varepsilon$ . This leaves  $D_F$  as the fractal dimension. Solving for  $D_F$  leaves the equation:

$$D_F = \log N / \log \varepsilon$$

FracLac plugin, a free add-on for ImageJ, allows for the calculation of fractal values using a number of existing algorithms and the ability to change multiple calculation settings (Karperien 2007).

### **2.5.1. Simple box count**

One such algorithm is the simple box count, which takes the slope of the above equation, determining the number of parts  $N$  changes with scale  $\varepsilon$  (calculated in this case as [box size/image size]) thus giving:

$$D_B = \text{the slope of } (\ln N / \ln \varepsilon)$$

Equation 3

$D_B$  is the box counting dimension. FracLac allows for the calculation of  $D_B$  based on parameter settings that determine how many different values of  $N$  and  $\varepsilon$  will be used (Karperien 2007). From a more visual standpoint, the algorithm lays a series of grids of decreasing box size over the image, and counts the number of boxes that contain portions of the image for each box size.

Box count, in addition to FD, also gives each image a value of lacunarity, which is a measure of texture; for example variability in pattern. An image that is closer to being homogenous and to having a translationally and rotationally invariant pattern will have a lower value of lacunarity, given as  $\lambda$ . Patterns with similar fractal dimensions can often be distinguished by their lacunarity, which is determined by the following, more complicated formula:

$$\lambda_{\varepsilon,g} = CV_{\varepsilon,g}^2 = (\sigma_{\varepsilon,g} / \mu_{\varepsilon,g})^2$$

Equation 4

where  $\lambda$  represents the lacunarity for each grid of caliber  $\varepsilon$  (as above) calculated from the standard deviation  $\sigma$  and mean  $\mu$  of pixels per box for each grid orientation  $g$  (grid orientation is the variable location of the box grid laid over the ROI).

We attempted to compare about the same number of images for the initial review of Test set 1 and Test set 2 which were produced by two independent investigators without training in histopathology. For each set, a total of 70 images were captured at 20X were analyzed using the simple box count. The FracLac settings for box counting used boxes that ranged from a minimum of two pixels in size to a maximum size of 45% of the ROI.

This procedure of calculating the fractal dimensions and lacunarity values using Image J was repeated throughout this study. The difference in fractal dimension and lacunarity values was recorded with the change in pathology diagnosis using the same software, with same hamster tissues images was also evaluated.

This study was carried out to confirm the repeatability and accuracy of the FD analysis method and the approach of using fractal dimensions to distinguish stages in experimental oral carcinogenesis.

### **2.5.2. Inflammatory Infiltrate Analysis**

In addition to simple FD based on POI analysis, an additional correlation with the density of inflammatory infiltrate cells that populate regions just below the epithelial layer was also examined. Though not strictly a fractal-based analysis, because of the area involved; an inflammatory infiltrate cell count is useful in pathology diagnosis of OSCC, and could potentially prove useful to improve FD analysis.

The inflammatory infiltrate was defined by populations of immune effector cells.



Cells counted were recognized using H+E staining and histopathology of lymphocytes, histiocytes (tissue type), and granulocytes (eosinophiles, basophiles, mast cells, and polymorphonuclear cells).

In order to perform this procedure, the RGB image of the slide was converted to greyscale as before, but this time the image was threshold to emphasize the inflammatory cells. These cells represented the portion of the image which would be the ROI for the cell count. From this point, the Analyze Particles feature in ImageJ could be used to count the cells and their sizes. This procedure was performed on a subset of the original group of images, yielding information including infiltrate cell count, infiltrate area, average infiltrate cell size, and area fraction of the image covered by infiltrate cells.

## **2.6. Immunohistochemistry:**

Immunohistochemistry was used to select cells in tissue sections that are present in a FD analysis. We tested the concept that some keratinocytes cells compared to other similar keratinocytes that form a mucosal pattern are more significant because of protein expression in this cells and this physiologic attribute results in a unique placement in the defining pattern to form the FD.

Method of detection: Standard methods diaminobenzadine and horse radish peroxidase to produce a blue black-brown precipitation following secondary anti rabbit, mouse as required (1:1000) (Schwartz 2000) Sodium citrate antigen retrieval with heat until boiling was reached and was used to enhance detection.

### **Antibodies:**

1. Mitogen Activated Phosphokinase: Anti-phospho-p38 (pThr<sup>180</sup>/pTyr<sup>182</sup>) antibody produced in rabbit; polyclonal antibody (Sigma Chemical-Aldrich, St. Louis, MO) (1:200 concentration used).
2. 8-Hydroxy-2'-deoxyguanosine: Mouse Anti-8-oxo-dG Monoclonal Antibody (clone 2E2); Trevigan, Gaithersburg, MD (1:100 concentration used)
3. Proliferating cell nuclear antigen (PCNA): Antibody to Mouse monoclonal (PC10), PCNA (Santa Cruz Biotechnology, Dallas, Tx) (1:200 concentration used)
4. CD44: Rabbit antibody, polyclonal (Millipore, Billerica, MA) (1:200 concentration used)

### **2.7. Data analysis**

IBM SPSS Statistics was used to process data for the image sets. Each image had its Pattern of Invasion listed based on the guide to pattern of tumor invasion (Brandwein-Gensler, Teixeira et al. 2005). The box count FD and box count lacunarity were listed, as well as the average FD and lacunarity taken as the arithmetic mean of all values.

The values we tabulated based on their predicted pattern of invasion and an Independent T-test was performed for values obtained from this study against the values from the previous study. The test was carried out to observe the presence of a statistically significance. In addition to this, the values obtained from both the sets were comparatively analyzed using Kappa Analysis using MedCalc Statistical Software. This analysis is used to calculate an inter-rater agreement statistic (Kappa) to evaluate the agreement between two classifications on ordinal or nominal scales (Cohen, 1960). Agreement is quantified by the Kappa (K) or Weighted Kappa (Kw) statistic (Fleiss et

al., 2003).  $K$  is 1 when there is perfect agreement between the classification system;  $K$  is 0 when there is no agreement better than chance;  $K$  is negative when agreement is worse than chance.

Along with the Kappa analysis, Correlation coefficients were also calculated for the fractal dimensions and lacunarity values. To determine the correlation between the variables, it was determined that a Spearman correlation would be performed. The Spearman rank correlation coefficient, given as  $\rho$  (and often referred to as Spearman's rho), is a non-parametric measure of statistical dependence for two variables, with a range from -1 to +1. A value of +1 indicates a perfect, monotonic correlation, whereas a value of -1 indicates a perfect, monotonic, negative correlation. A value of 0 indicates no correlation at all. Determining the most correlated variables will allow a hierarchical cluster process to be performed, making it possible to accurately determine POI of a tissue image based on multiple variables (Sarstedt and Mooi 2010).

FD values were compared using multiple variable graphs to determine a difference in FD as the diseases progresses.

To enhance the diagnosis, we carried out Independent T-tests between the stages within the various stages of carcinogenesis. Fractal dimension data from contiguous stages of development were compared with each other to observe the presence of a significant difference. This analysis can predict the incorporation of fractal dimension values as a diagnostic tool.

In addition, inflammatory infiltrate values were added. Specifically the total cell (whole particle) count for the ROI, the total area covered as part of the ROI, average cell size within the ROI, and the area fraction, determined as the percentage of pixels counted as

infiltrate within the ROI (Rasband 2009). Average Fractal dimension values were calculated for each of the variable and were tabulated against the stages of oncogenesis .i.e. Normal, Dysplasia and Severe stages. The response of the infiltrate variables to the disease progression is analyzed.

### **3. RESULTS**

#### **3.1 Rationale:**

Histopathology diagnosis for premalignant dysplasia and/or oral squamous cell carcinoma (OSCC) has in a significant manner been incorrect or variable among similarly trained pathologists. Furthermore some studies have demonstrated that the same pathologist will offer different diagnoses for the identical tissue specimen. Clearly there is a need for diagnostic accuracy and improvement of precision.

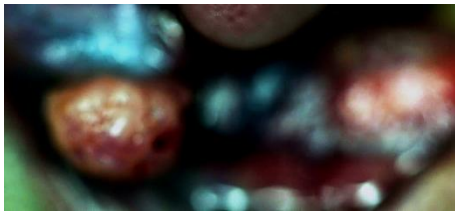


Figure 1: DBP Induced Cancers in Golden Syrian Hamster

Fractal dimension (FD) analysis is a mathematical attempt to apply precision to diagnosis by the pathologist with an improvement of pattern recognition. FD as documented in the introduction has been reported as changed during presentation of human oral squamous cell carcinomas (OSCC) and other oral keratotic diseases (need ref here). However to our knowledge there has been no attempt to demonstrate whether FD analysis can be used to improve accuracy of diagnosis of oral diseases such as premalignant change, dysplasia or OSCC through a well- controlled experimental model for oral carcinogenesis (Figure 1.) Use a systematic approach, for example box counting under different conditions, and a comparison by two independent investigators which are untrained as to histopathology diagnosis to evaluate use of FD analysis to improve accuracy of histopathology diagnosis for OSCC.

#### **3.2. Experimental Oral Carcinogenesis Model**

Details for the experimental oral carcinogenesis design are described in the Methods Section. Oral carcinogenesis is induced through a repeated application of the type I

(WHO) carcinogen, dibenz [a, l] pyrene (0.025 mM, dissolved in acetone (1%, v/v): about 2.5 nM/application for 3X/wk for 25 weeks). We recorded induction in 20/20 Syrian hamsters (*Mesocricetus auratus*) invasive OSCC in the floor of mouth compared to a acetone control application to the identical tissue. There was determined to be a highly significant ( $p > .0001$ ) difference between these two groups.

Presence of these tumors were confirmed using paraffin embedded tissue section (5-6 micron thin); with staining of sections with hematoxylin (Mayer's) and eosin for standard histopathology diagnosis.

### **3.3. Histopathology Criteria for Assessment of Pathology**

Epithelial mucosa changes were essential to establish the initial diagnosis the criteria are consistent with squamous intraepithelial neoplasia (SIN) described by WHO consensus as described in the Methods Section. In brief, normal, or mild, moderate and severe dysplasia and OSCC changes in oral epithelium are assessed by the presence features which accumulate in number and severity as pathology progresses from normal, through dysplasia to OSCC. Some of these features include: hyperkeratosis, hyperplasia, anaplasia, dyskeratosis, hyperchromatism, mitoses, chromatin clumping were used here to designate normal, dysplasia and OSCC.

### **3.4. Oral Epithelial Mucosa Architecture Changes During Oral Carcinogenesis**

Using Brandwein criteria as noted in the Methods Section we have designated the types of changes as patterns of invasion (*POI*). These include (1) broad invasive front; (2) finger like front; (3) tumor islands; islands (>15 cells) and (4) satellites more than 1mm

from the tumor front (Figure 2). These patterns of mucosa invasion (*POI*) are used through our FD analysis for our results.

Brandwein's criteria also include the histopathology recognition of an inflammatory infiltrate which is also noted below and included in our FD analyses.

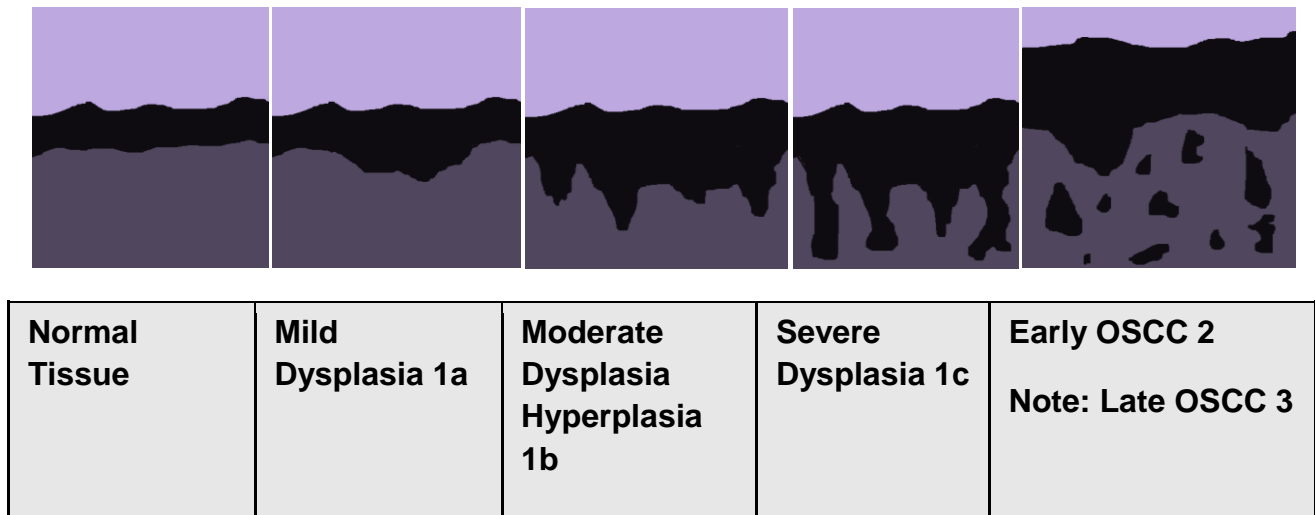


**Figure 2: A Modification of Brandwein's Patterns for Invasion for (*POI*) OSCC**

### **3.5. Conversion of Histopathology to a Fractal Dimension Analysis**

In previous studies an effort was made to improve upon the FD analytic capability of the software Image J. Therefore, our comparisons will use Image J as a standard for FD analysis for each tissue image at a 20X magnification.

Values from **test set 1** and **test set 2** were attained as two independent evaluations by two different individuals using identical histopathology images. A **test set 3** was also evaluated by a single investigator as used to assess individual variability.

### **3.6 A series of comparisons were used to test accuracy of FD analysis**

These were:

- 1) A comparison between **test set 1** and **test set 2** using FD analysis and *POI*
- 2) A comparison between **test set 1** and **test set 2** using FD analysis in conjunction with assessment of an inflammatory infiltrate (*II*)
- 3) A comparison between **test set 1** and **test set 2** using FD analysis with consideration of Lacunarity (*Lac*) or shape deformation of pattern developed through FD expression.
- 4) An evaluation of inter-individual variation in FD analysis using **test set 3**.
- 5) Further attempt to increase precision of FD analysis for a test set (3) using immunohistochemical evaluations.
- 6) Our rationale was to test increase in accuracy in diagnosis with a selective staining/ protein expression. We also tested:
  - to evaluate the requirement for a H+E standard histopathology slide to obtain a FD analysis.
  - to evaluate distribution of stain/protein expression was required for FD analysis.

This was achieved using *markers that were used for this test are expressed in basal and supra basal layers of mucosa* (proliferating cell nuclear antigen (PCNA); basal and progenitor cell: CD44).

- a. Stained tissue sections for a selective protein expression evaluated with an H+E standard slide for histopathology assessment and FD (+/- *POI* +/- *II*).



- b. Stained tissue sections for a selective protein expression evaluated with contiguous H+E standard slide for histopathology assessment and FD (+/- *POI +/- II*).

This was achieved using *markers that were used for this test are expressed at all layers of mucosa* (mitogen activated phosphokinase (MAPK); 8-oxo-deoxyguanosine (dG):

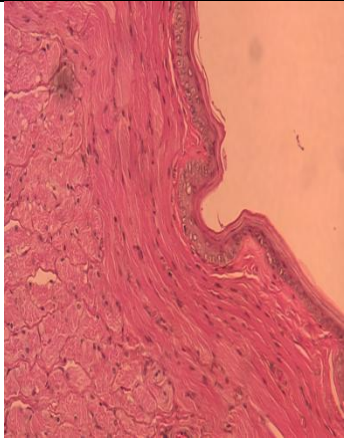
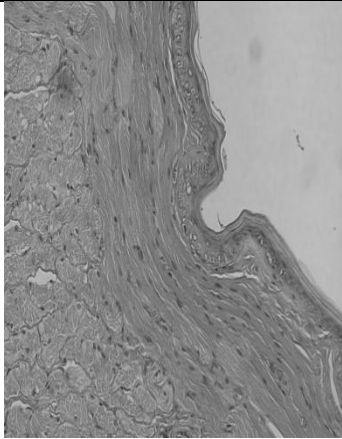
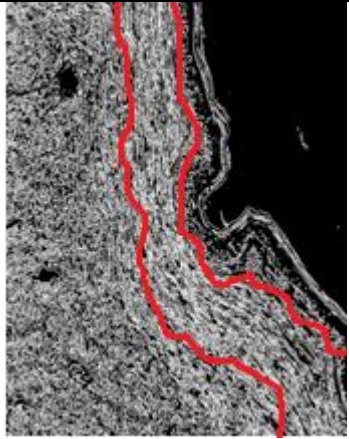
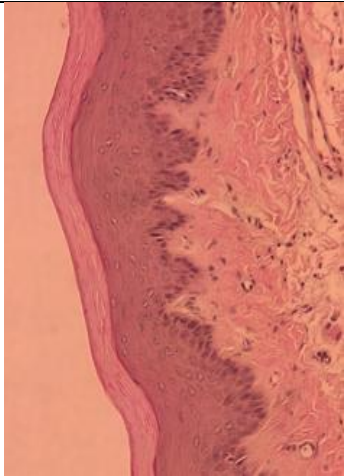
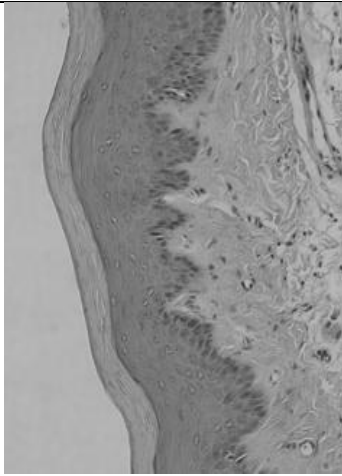
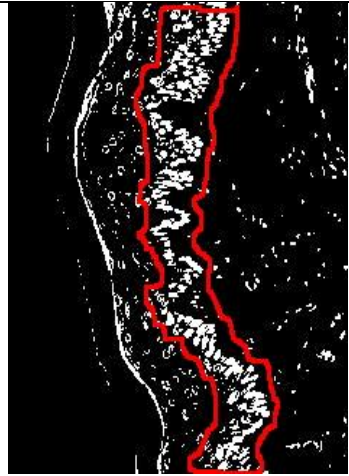
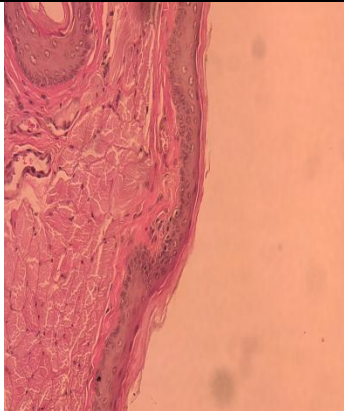
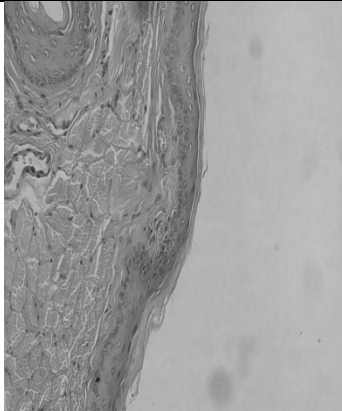
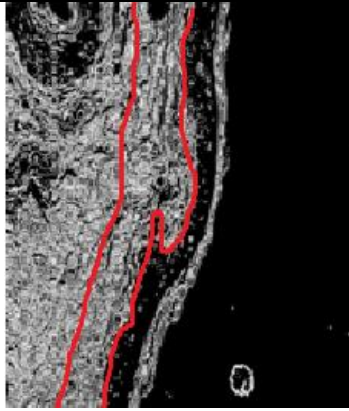
- c. Stained tissue sections for a selective protein expression evaluated without an H+E standard slide for histopathology assessment and FD (+/- *POI +/- II*)
- d. These stained tissue sections for a selective protein expression were evaluated with an H+E standard slide for histopathology assessment and FD (+/- *POI +/-*).

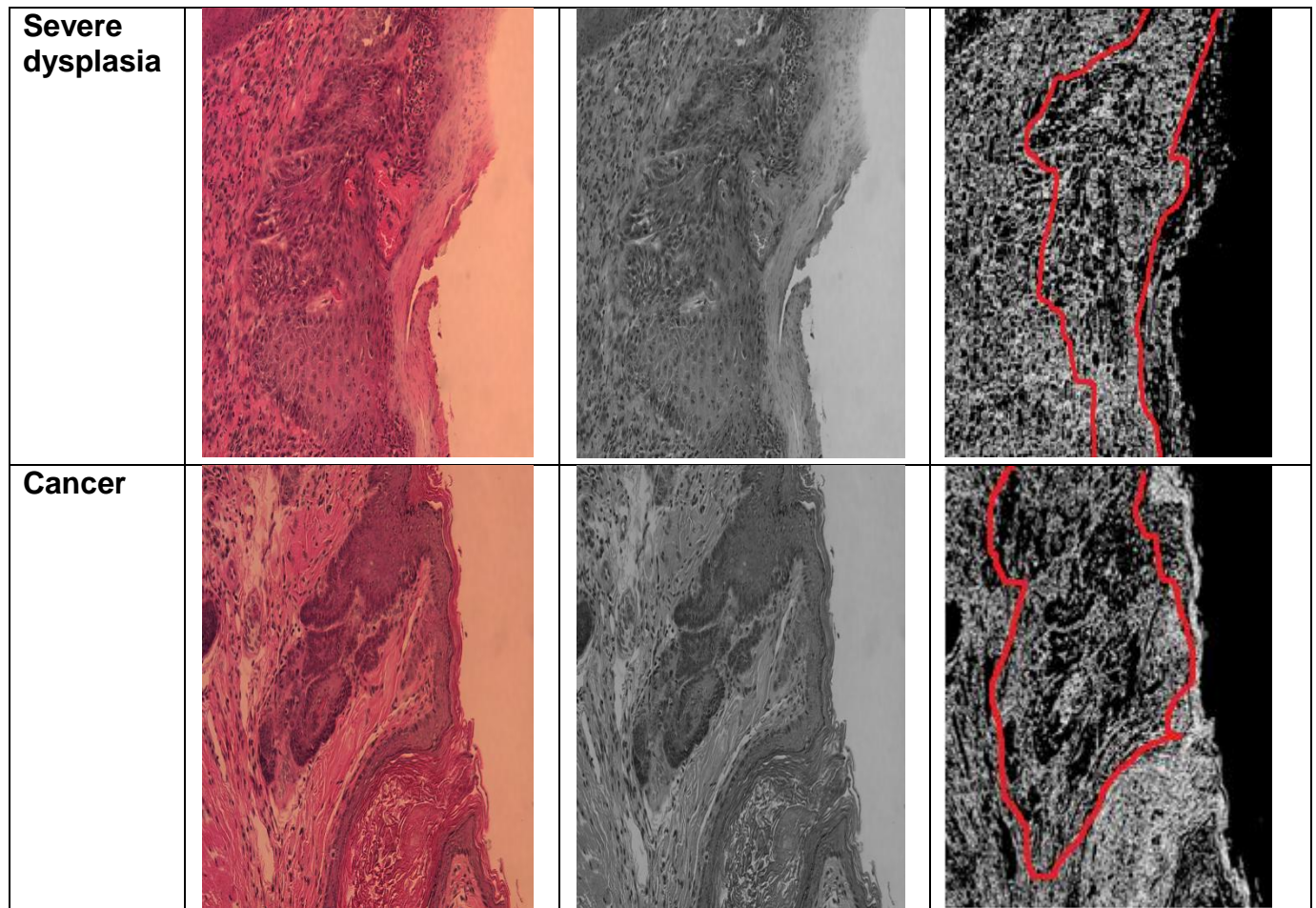
Other considerations for accuracy include a determination of the area of invasion front of epithelial –mesenchymal interface between tissues and this is reflected in the FD values obtained and considered in the conversion of histopathology to FD image (Figure 3.) as we proceed from normal, through dysplasia to OSCC.

Histopathology criteria included: in fractal dimension analysis were

- 1) Brandwein's Pattern of Invasion (ref)
- 2) Inflammatory infiltration presence or absence

**Figure 2: Conversion process of digital slides through steps: 1, original image; 2, greyscale; 3, threshold to emphasize epithelial layer.**

	1. Original Image	2. Grey Scale	3. Binary Image
<b>Normal</b>			
<b>Mild Dysplasia</b>			
<b>Moderate Dysplasia</b>			



### **3.6.1 Fractal Dimension Analysis to Assess Difference between Test 1 and Test 2 of an Identical Set of Histopathology Photo images of Histopathology**

Stated above is our goal to achieve improved accuracy for FD analysis. To accomplish this we compared (See Table 1.) as indicated above two independent examinations using FD analysis occurred using the identical tissue sections and photomicrographs for a selected gated area (**Test set 1 and Test set 2**).

**Table 1: Test Set 1: DBP treated Group (Test Group 1)**

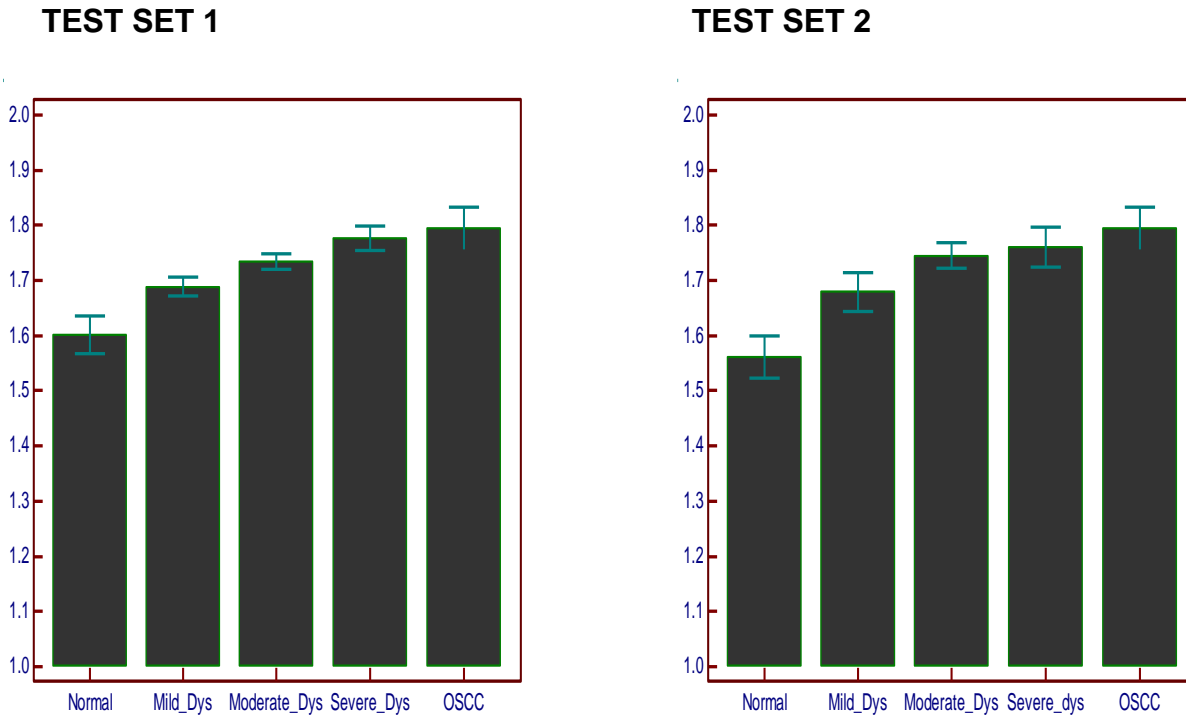
<b>Normal</b>	<b>Mild Dysplasia</b>	<b>Moderate Dysplasia</b>	<b>Severe Dysplasia</b>	<b>OSCC</b>
1.58	1.66	1.76	1.76	1.82
1.45	1.58	1.75	1.66	1.72
1.52	1.74	1.81	1.76	1.80
1.53	1.74	1.77	1.78	1.82
1.49	1.64	1.73	1.75	1.83
1.61	1.63	1.74	1.68	1.92
1.60	1.71	1.74	1.81	1.75
1.58	1.73	1.75	1.77	1.81
1.63	1.69	1.67	1.81	1.75
1.62	1.64	1.75	1.74	1.78
1.57	1.71	1.73	1.84	1.74

**Table 2: DBP treated Group (Test Group 2)**

<b>Normal</b>	<b>Mild Dysplasia</b>	<b>Moderate Dysplasia</b>	<b>Severe Dysplasia</b>	<b>OSCC</b>
1.5777	1.688	1.715	1.762	1.82
1.4739	1.6386	1.716	1.762	1.72
1.5826	1.662	1.717	1.764	1.80
1.5709	1.674	1.727	1.773	1.82
1.6179	1.681	1.729	1.853	1.83
1.627	1.6829	1.729	1.764	1.92
1.6348	1.702	1.732	1.762	1.75
1.648	1.703	1.741	1.816	1.81
1.6279	1.709	1.741	1.8	1.75
1.6	1.71	1.749	1.738	1.78
1.658	1.6911	1.758	1.75	1.74

Presented above are the FD analysis results. Next we compared these results to determine statistical significance difference between the sets.

**Fig 4: Multiple variable graphs of Test 1 and Test 2**



The values obtained from Test 1 compared to Test 2 are presented and analyzed statistically. A T-test was performed separately from test 1 and test 2 for normal, dysplasia (mild, moderate, severe) and OSCC (p-values > 0.05).

Results demonstrate that the process of FD analysis in conjunction with Brandwein's criteria (POI and inflammatory infiltrate assessment) is repeatable with little significant variability between independent investigators using the identical images.

**Table 3(a): T-test (assuming equal variances) for OSCC**

	OSCC_1	OSCC_2
Sample size	11	11
Arithmetic mean	1.7945	1.7945
95% CI for the mean	1.7570 to 1.8321	1.7570 to 1.8321
Variance	0.003127	0.003127
Standard deviation	0.05592	0.05592
F- test for equal variances	P = 1.000	
Standard error of the mean	0.01686	0.01686

Difference	0.0000
Standard Error	0.02385
95% CI of difference	-0.04974 to 0.04974
Test statistic t	0.000
Degrees of Freedom (DF)	20
Two-tailed probability	P = 1.0000

**Table 3(b): T-test (assuming equal variances) for Normal tissues**

	Normal_1	Normal_2
Sample size	11	11
Arithmetic mean	1.5618	1.6017
95% CI for the mean	1.5232 to 1.6004	1.5673 to 1.6361
Variance	0.003296	0.002622
Standard deviation	0.05741	0.05121
Standard error of the mean	0.01731	0.01544

F-test for equal variances	P = 0.725
----------------------------	-----------

Difference	0.03988
Standard Error	0.02320
95% CI of difference	-0.008505 to 0.08827
Test statistic t	1.719
Degrees of Freedom (DF)	20
Two-tailed probability	P = 0.1010

**Table 3(c): T-test (assuming equal variances) for Dysplasia**

	Dysplasia_1	Dysplasia_2
Sample size	33	33
Arithmetic mean	1.7304	1.7294
95% CI for the mean	1.7127 to 1.7480	1.7102 to 1.7485
Variance	0.002467	0.002916
Standard deviation	0.04967	0.05400
Standard error of the mean	0.008646	0.009401

F-test for equal variances	P = 0.639
----------------------------	-----------

Difference	-0.0009798
Standard Error	0.01277
95% CI of difference	-0.02650 to 0.02454
Test statistic t	-0.0767
Degrees of Freedom (DF)	64
Two-tailed probability	P = 0.9391

**The P-value > 0.05, thus difference between both the tests is statistically insignificant.**



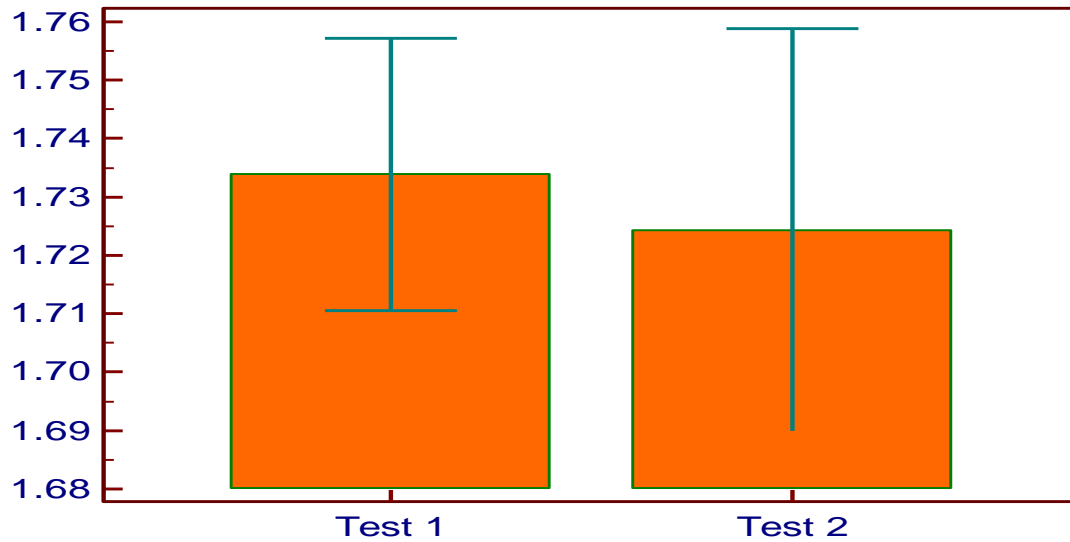


**Figure 5: The graph shows an insignificant difference of 0.0095 between the Fractal dimension values from Test 1 and Test 2.**

### **Kappa Value Analysis for Agreement between Two Individuals**

To give additional information about the consistency of the approach, an inter-individual-rater agreement test was performed on the values obtained from Test set 1 verses Test set 2. The analysis gives a Kappa value (K), which determines the evaluation agreement between two classifications on ordinal and nominal scales. When K is 1, there is perfect agreement between the system; When K is 0, there is no agreement better than chance; K is negative when agreement is worse than chance. A Kappa (K) value of 0.488 is obtained, which can be assessed to be a fair strength of agreement between the values of Test set1 and Test set 2.

### 3.6.2. Inflammatory Infiltrate and Brandwein Criteria

Another important characteristic in the Brandwein criteria is the inflammatory infiltration found in tissues during oral carcinogenesis. Inflammatory infiltration although heterogeneous in nature can provide a prognostic and histopathology criteria for OSCC. The inflammatory infiltration of various types of immune cells increase during oral carcinogenesis as shown in figures 3 and 4 is derived from **Test set 1**.

Values for the inflammatory cells were assessed in an identical manner for **Test set 2** and calculated for the POI stage of hamster oral carcinogenesis. Both sets of FD analyses therefore shown a pattern of increase in inflammatory infiltration associated with increases in histopathology associated with exposure to DBP and induction of oral carcinogenesis (Figure 4.).

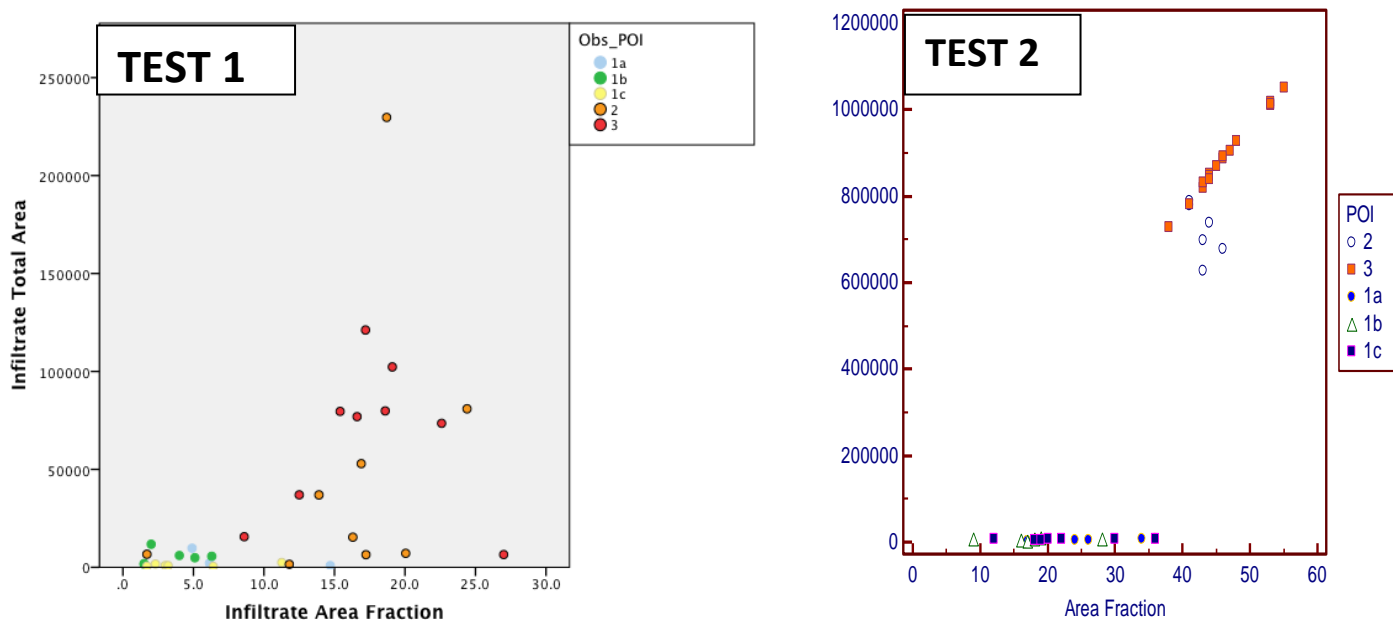


**Figure 6: Correlation (Test set 1 and Test set 2) of Total area of the infiltrate and Area fraction with the POI**



For Test set 2 inflammatory infiltration values are tabulated as follows in table 4. In this Test set of data we compared the size and estimated numbers of inflammatory cells in a 20X magnified photo image of a H+E tissue section that was previously used to establish a FD analysis based on the modified Brandwein's patterns of invasion (POI). Table 4 data shows there was a gradual progression of inflammation infiltration into the tissues examined for changes in dysplasia and OSCC.

**Table 4: Inflammatory Infiltrate data for Test set 2:**

	<b>Count</b>	<b>Total area</b>	<b>Average size</b>	<b>Area fraction</b>
<b>Normal</b>	16.59	5326.768	25.86	27.72
<b>Mild</b>	21.28	6479.32	59.96	16.82
<b>Moderate</b>	30.55	6333.3	65.16	20.05
<b>Severe</b>	364.67	64315.9	124.24	43.31
<b>Cancer</b>	1424.84	89266.7	135.74	49.78

Moreover, in numbers of inflammatory cells and the average size of cells increase explicitly, with a sharp increase in area fraction and total area of infiltrate content during moderate dysplasia. This is expected to be an important discriminator for oral carcinogenesis once further studies are performed and these results show that FD analysis in conjunction with Brandwein criteria POI can assist in a dissociation of normal, types of dysplasia and OSCC.

Spearman Correlation coefficient calculated for total infiltrate area (area covered by infiltrate cells) against POI for Test 1 and Test 2 is 0.676 and 0.6892 respectively. This shows that the correlation with respect to POI is equivalent when carried out by both the investigators.

**Table 5: T-test (assuming equal variances) for Inflammatory Infiltrate Data from Test 2**

	<b>Total Area</b>	<b>Cell size</b>	<b>Cell count</b>
<b>Difference</b>	9306.7576	-17.272	25.5838
<b>Standard Error</b>	22282.2242	332.7075	21.7161
<b>95% CI of difference</b>	-42076.14 to 60689.65	-784.49 to 749.95	-24.49 to 75.66
<b>Test statistic t</b>	0.418	-0.0519	1.178
<b>Degrees of Freedom (DF)</b>	8	8	8
<b>Two-tailed probability</b>	P = 0.6872	P = 0.9599	P = 0.2726

A T-test was performed separately from test 1 and test 2 for Total infiltrate area, Average cell size and Cell count (p-values > 0.05). This test confirms our previous statement of consistent results for FD among independent investigators.

### **3.6.3. Assessment of Fractal Dimension (FD) Pattern, Lacunarity Characteristic**

FD analysis can be performed using characteristics such as Lacunarity. This characteristic is an internal indicator of the variability of the FD box counting procedure that is derived from the pattern that describes the epithelia-mesenchymal interface where invasive carcinoma is observed to form. Lacunarity also gives an estimated value for the completeness of the fractal dimension pattern as a product of a tissue section which can present with incomplete cells or variations in staining.

In addition to Fractal dimension, Lacunarity values were also calculated using the FracLac Plugin. To determine the correlation between fractal dimension value and the lacunarity, a spearman rank test was carried out between the fractal dimension and Lacunarity. Spearman's coefficient of rank correlation ( $\rho$ ) of -0.838 was obtained in a box plot of FD versus Lacunarity, determining a strong negative correlation between them. Because of the strong correlation between the two variables, a scatter plot of

Fractal dimension values against the lacunarity which were grouped based on their pattern of invasion (POI) was created.

The cancerous cells were found to be clustered near the regions of high FD and low Lacunarity, whereas, the dysplasia was found concentrated in the regions of medium lacunarity and fractal dimensions. The normal cells were clustered near high lacunarity and low FD. This plotting show that precision of FD associated with degrees of Lacunarity can be harnesssed to differentiate between normal cells, dysplasia and cancer cells (Figure 5).

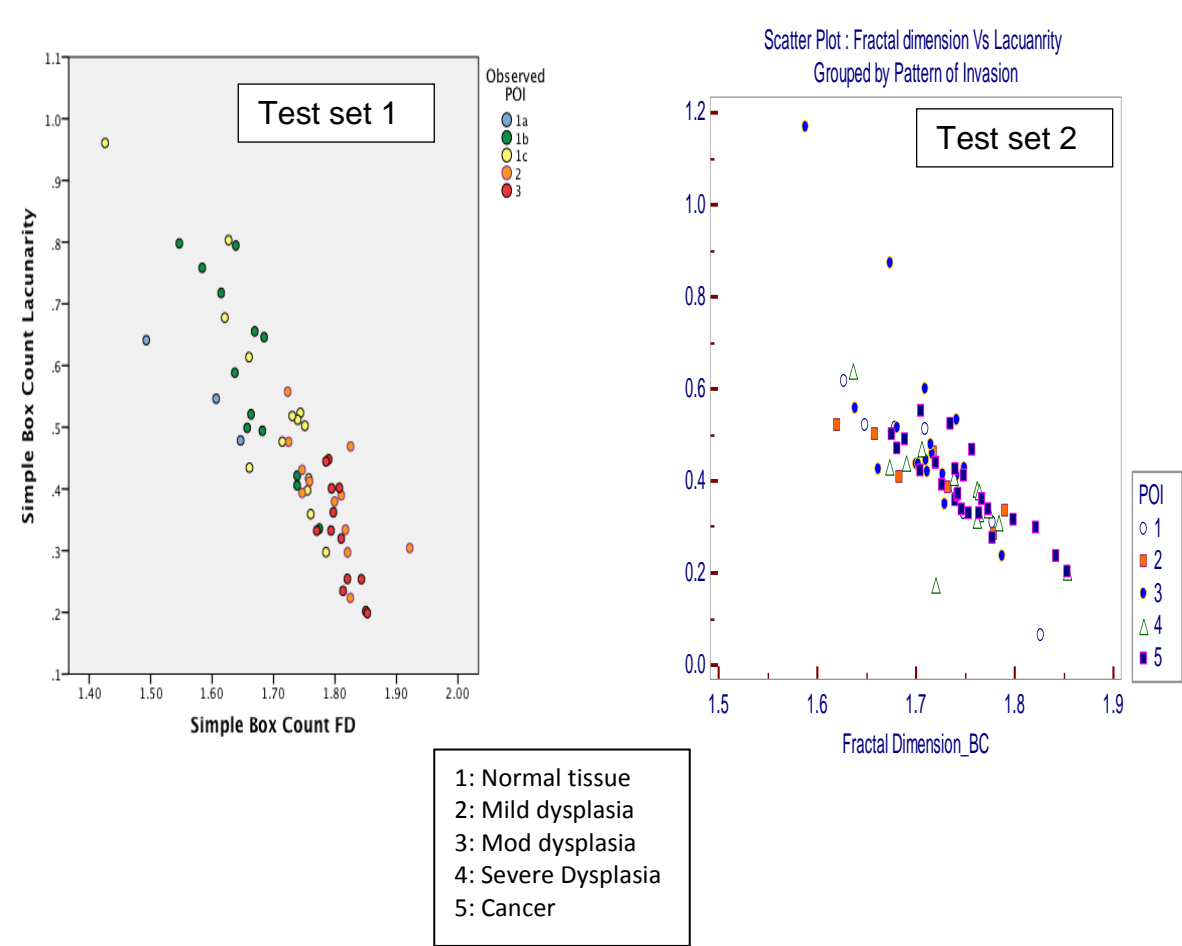


**Figure 7: Scatter plot with Fractal dimension (Simple box count) Vs Lacunarity (Simple box count) grouped with respect to POI**

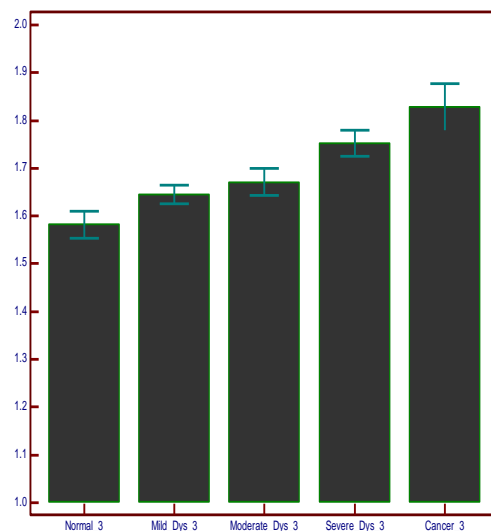
### **3.6.4. Assessment of Variability of FD Analysis to Evaluate Inter-Individual Variation: Comparison between Test set 2 and Test set 3**

#### **FD Analysis for Test Set 3**

This group of tissues forming **Test set 3** included a hematoxylin and eosin stained tissue slides. We again used Brandwein's criteria (POI and inflammatory infiltration) as stated above and compared the results with Test set 2 which was produce by the identical investigator.

**Table 6: DBP Treated Group (Test set 3)**

Normal-3	Mild-Dys-3	Moderate-Dys-3	Severe-Dys-3	Cancer-3
1.5	1.6	1.66	1.78	1.92
1.62	1.642	1.67	1.74	1.874
1.56	1.647	1.68	1.68	1.815
1.55	1.62	1.7	1.74	1.917
1.59	1.63	1.75	1.79	1.772
1.62	1.64	1.68	1.73	1.796
1.59	1.64	1.69	1.75	1.856
1.62	1.67	1.61	1.76	1.8067
1.56	1.68	1.63	1.74	1.8294
1.61	1.69	1.644	1.82	1.7



An inter-individual-rater agreement test was performed on the values obtained from **Test set 2** verses **Test set 3**. The analysis gives a Kappa value (K), which determines the evaluation agreement between the two sets as well as **Test set 1**. A Kappa value of 0.301 is obtained which can be determined as a fair value of agreement between the sets.

**Table 7: Independent T-test results for Test set 2 and Test set 3**

	<b>Normal</b>	<b>Dysplasia</b>	<b>Cancer</b>
<b>Difference</b>	-0.01407	0.0264	0.02861
<b>Standard Error</b>	0.02019	0.0161	0.02758
<b>95% CI of difference</b>	-0.05649 to 0.02835	-0.007424 to 0.06022	-0.02933 to 0.08655
<b>Test statistic t</b>	-0.697	1.64	1.037
<b>Degrees of Freedom (DF)</b>	18	18	18
<b>Two-tailed probability</b>	P = 0.4948	P = 0.1184	P = 0.3133

Similar to the previous analysis, the values obtained from **Test set 2** compared to **Test set 3** are analyzed statistically using an independent sample T-test. It was carried out separately from **Test set 2** and **Test set 3** for normal, dysplasia and OSCC which displayed high P values ( $p\text{-values} > 0.05$ ), proving that the difference between both the sets have no statistical significance.

The inflammatory infiltrate data is taken into consideration to compare the average size, fraction and the inflammatory cells this tissue **Test set 3**. A plot is drawn to determine the correlation between area fraction and the total area of the infiltrate. The plot displays a similar pattern to **Test set 2** results. The total area of the infiltrate has a positive correlation with the POI, with a Spearman coefficient of 0.733 ( $P < 0.001$ ).

In addition to this, the correlation between fractal dimension value and the Lacunarity of the test data set 3 was analyzed. A spearman rank test was carried out between the fractal dimension and Lacunarity giving a rank correlation ( $\rho$ ) of  $-0.884(P < 0.001)$  was obtained in a box plot of FD versus Lacunarity, determining a strong negative correlation between them. The cancerous cells were found to be clustered near the regions of high FD and low Lacunarity, whereas, the dysplasia was found concentrated in the regions of medium Lacunarity and fractal dimensions. The normal cells were clustered near high Lacunarity and low FD. This pattern is similar to the scatter plot generated from **Test set 2**.

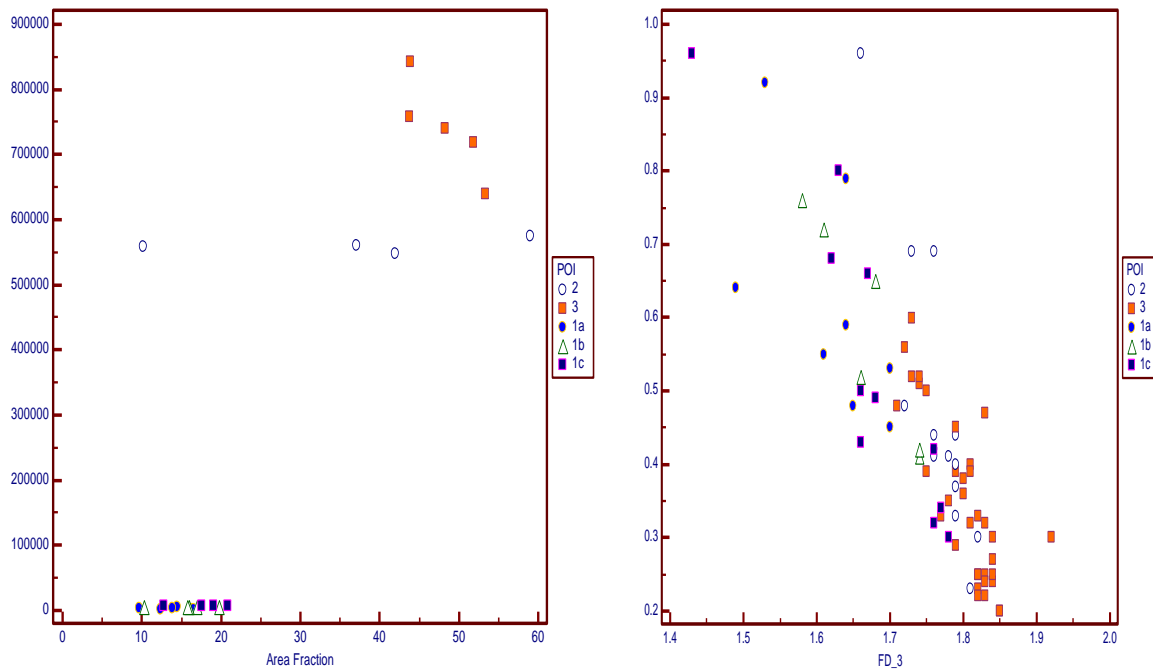


**Figure 8: TEST SET 3 DATA: (a): Inflammatory infiltrate scatter plot with total area plotted against area fraction; (b): Spearman correlation scatter plot with Lacunarity versus Fractal dimension to determine their relation with POI.**

### **3.6.5. Inter-Data Differentiation of the stages of Cancer development of Oral carcinogenesis in Data set 3**

To determine the differentiation in Mild dysplasia, Moderate dysplasia and severe dysplasia, a T-test was done for tissues. Differentiation between Normal-Mild dysplasia, Mild-Moderate-Severe & Severe dysplasia-OSCC tissues are statistically confirmed using this analysis.

**Table 8: Inter-data T-test for Test set 3:**

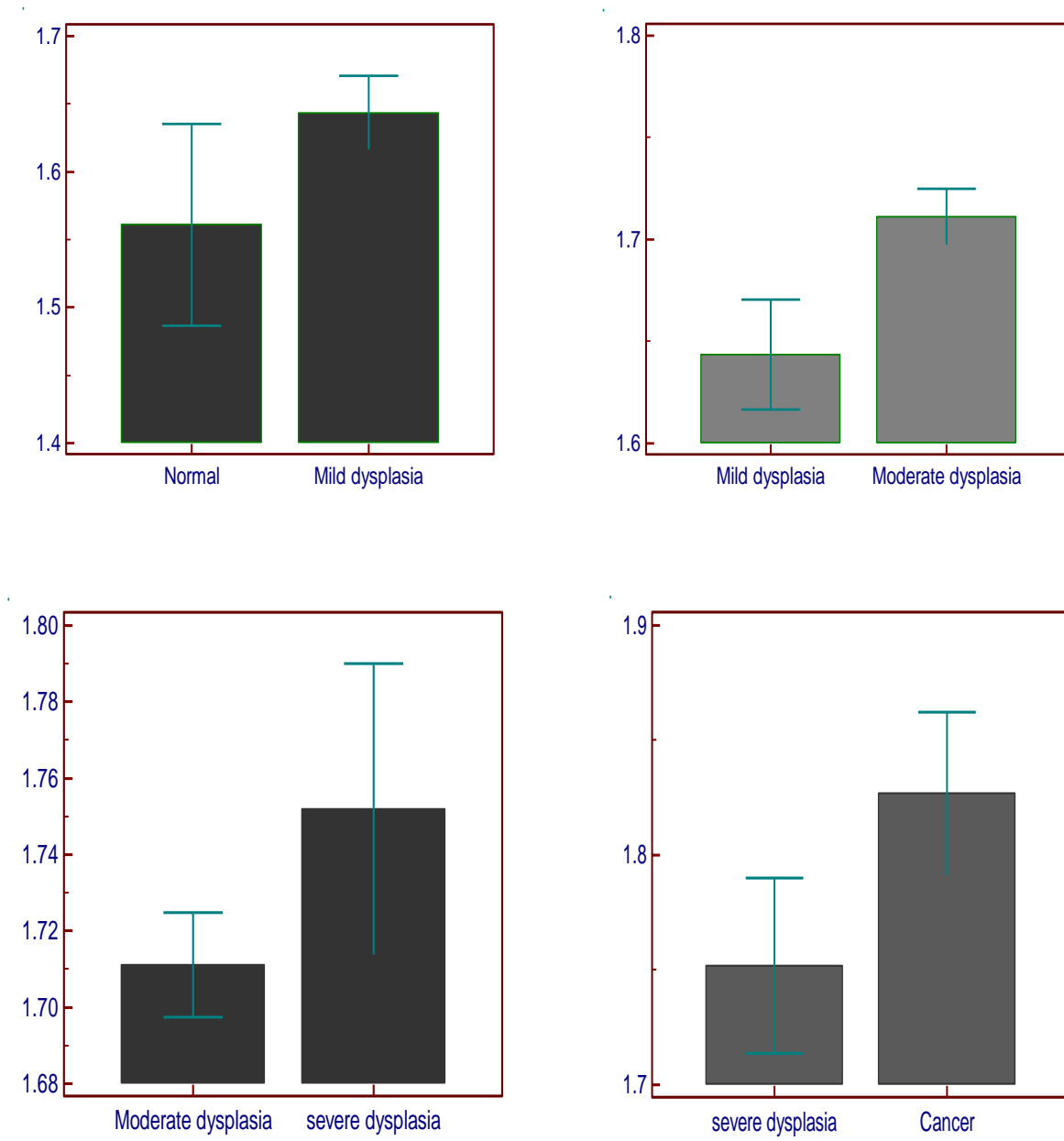
#### **Analysis between difference stages of cancer development**

**T-test (assuming equal variances)**

	<b>Normal-Mild Dysplasia</b>	<b>Mild Dysplasia- Moderate Dysplasia</b>	<b>Moderate- Severe Dysplasia</b>	<b>Severe Dysplasia- Cancer</b>
<b>Difference</b>	0.08247	0.06748	0.04083	0.07487
<b>Standard Error</b>	0.03343	0.01195	0.01757	0.0235
<b>95% CI of difference</b>	0.010 to 0.15	0.042 to 0.092	0.004 to 0.077	0.026 to 0.12
<b>Test statistic t</b>	2.467	5.646	2.324	3.187
<b>Degrees of Freedom</b>	14	18	21	21
<b>Two-tailed probability</b>	P = 0.0272	P < 0.0001	P = 0.0302	P = 0.0044

Low values of P are observed ( $P < 0.05$ ), thus proving that the differences are statistically significant.

**Fig 9: Comparison between Stages during Oral Carcinogenesis.**





### **3.6.6. FD Analysis in Immunohistochemistry Stained Tissue Sections**

In this study, FD analysis is dependent on a clear and precise placement of the interface between epithelium and underlying mesenchyme. We tested a dependence of FD upon protein expression obtained through IHC with a hematoxylin and eosin stained section but not of a contiguous nature.

The initial marker selected for initial review was PCNA because it can be used to designate cells in the basal or lower areas of the mucosa. Stated above this region is of importance to localize FD analysis and show an epithelial-mesenchyme interface.

**Table 9: PCNA Marker (Marker 1)**

Normal	Mild Dysplasia	Moderate Dysplasia	Severe Dysplasia	Cancer
0.8623	1.3884	1.6673	1.7397	1.792
1.2057	1.4672	1.675	1.7477	1.774
1.2144	1.4783	1.6884	1.689	1.815
1.4265	1.5358	1.7017	1.741	1.717
1.4298	1.3916	1.7558	1.793	1.772
1.3075	1.4895	1.6818	1.7308	1.796
1.128	1.54	1.6941	1.7531	1.856
1.47	1.67	1.611	1.7626	1.8067
1.56	1.68	1.6391	1.745	1.8294
1.23	1.62	1.644	1.723	1.7

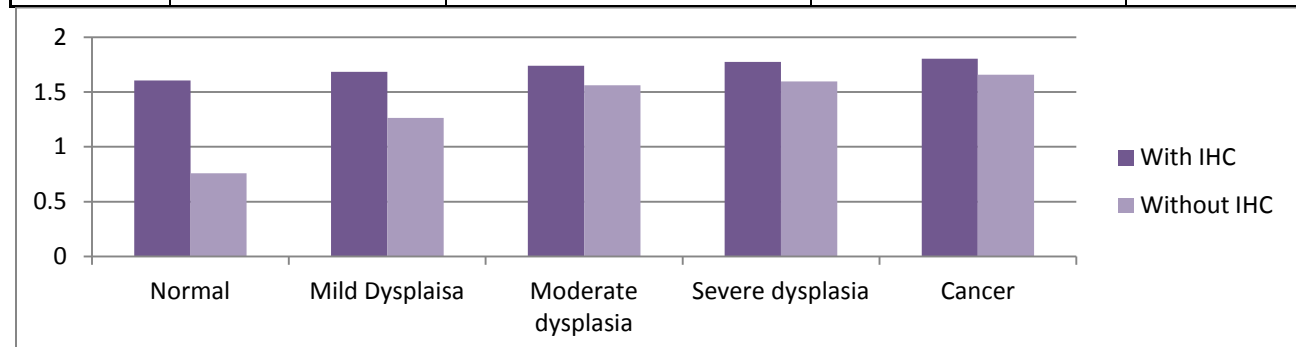


**Figure 10: The difference in fractal dimensions with the addition of stem cell markers can be observed. The FD values increased with the markers.**

Shown above the analysis indicated that this IHC marker (PCNA nuclear designation among basal and basal related keratinocytes) enhanced FD analysis through a better placement of an epithelial-mesenchymal interface and a possible tumor invasion front.

Differentiation between the tissues with mild dysplasia, moderate dysplasia and severe dysplasia were enhanced when the individual groups of tissues were subjected to stem cell markers evaluation.

**Table 10: Distinguishing the Normal tissues from Mild dysplasia, Mild dysplasia from Moderate dysplasia and Moderate dysplasia from severe dysplasia by the addition of PCNA (nuclear marker).**

	<b>Normal-Mild</b>	<b>Mild-Moderate</b>	<b>Moderate-Severe</b>	<b>Severe dys-Cancer</b>
<b>Difference</b>	0.1243	0.1068	0.06314	0.0614
<b>Standard Error</b>	0.05367	0.02774	0.0139	0.02559
<b>95% CI of difference</b>	0.010 to 0.23	0.047 to 0.16	0.032 to 0.093	0.006 to 0.116
<b>Test statistic t</b>	2.317	3.85	4.544	2.399
<b>Degrees of Freedom (DF)</b>	16	14	12	14
<b>Two-tailed probability</b>	P = 0.0341	P = 0.0018	P = 0.0007	P = 0.0309

This group of tissues formed Test set 3 and included a hematoxylin and eosin stained tissue slide and a contiguous stained immunohistochemical stained tissue section from normal (control) and DBP exposed floor of mouth tissue obtained following oral carcinogenesis.

Our second marker compared PCNA to a basal-stem like progenitor marker, CD44.

Specific histopathology was examined to compare PCNA (contiguous vs. non-contiguous H+E stained section) to CD44 (contiguous vs. non-contiguous H+E stained

slide). Availability of contiguous tissue sections helps to address the need for an H+E stained slide, or an H+E stained slide followed by IHC stained to increase accuracy for FD.

**Table 11: Comparison of Contiguous sections & Non-contiguous sections stained with Stem cell marker CD44.**

	<b>Contiguous CD44</b>	<b>Non-contiguous CD 44</b>
<b>Normal</b>	1.675	1.636
	1.680	1.692
	1.658	1.626
	1.660	1.614
	1.773	1.593
	1.629	1.640
	1.640	1.635
	1.674	1.634
<b>Dysplasia</b>		
	1.660	1.700
	1.773	1.750
	1.731	1.690
	1.727	1.651
	1.731	1.732
	1.744	1.641
	1.727	1.694
<b>OSCC</b>		
	1.946	1.752
	1.800	1.758
	1.847	1.731
	1.831	1.675
	1.831	1.680
	1.795	1.707
	1.705	1.702
	1.822	1.715

**Figure 11: Comparison of Contiguous sections & Non-contiguous sections stained with Stem cell marker CD44**

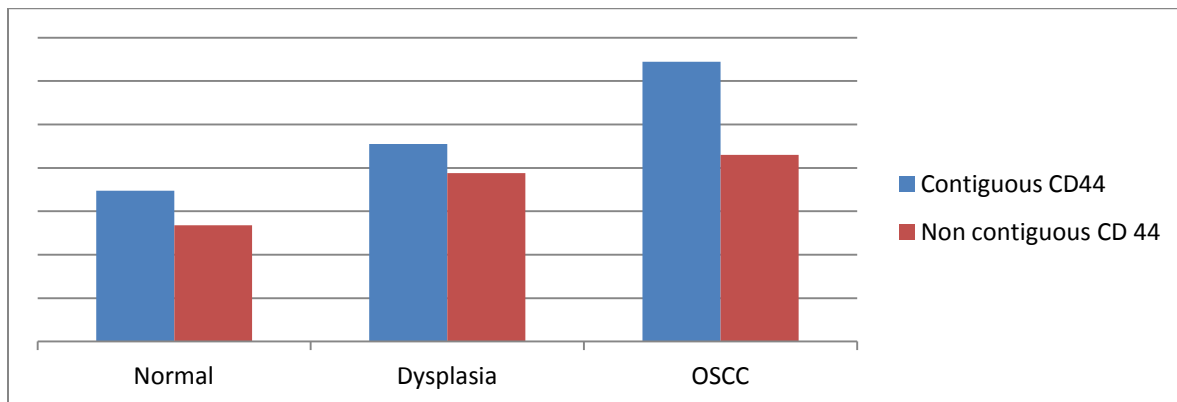


**Table 12: Paired sample t-test for determining significant contiguous tissues with PCNA and CD 44 markers.**

Mean difference	-0.02626
Standard deviation	0.05411
95% CI	-0.05158 to -0.0009352
Test statistic t	-2.17
Degrees of Freedom (DF)	19
Two-tailed probability	P = 0.0429

Contiguous Images with PCNA markers (H+E) and CD 44 markers gave much more significance than the images of PCNA & CD44 which were not contiguous.

Paired sample T-test showed a low P-value ( $P < 0.05$ ) thus the difference is statistically significant.

**Marker 3:** Mitogen activated phosphokinase is a maker for cell signals required for epithelial cell differentiation. This marker and 8-oxo-dG are expressed in cells distributed in all layers of oral mucosa. These markers did not have an H+E stained tissue section. Therefore FD analysis was based on only expressions.

**Table13: Marker 3: MAPK Expression**

Normal	Mild dysplasia	Moderate dysplasia	Severe Dysplasia	Cancer
1.17621	1.356	1.6157	1.74049	1.834
0.8801	1.43	1.6308	1.755	1.8353
0.9753	1.39	1.6388	1.8008	1.8484
1.0013	1.4327	1.6462	1.8307	1.8647
1.23	1.4405	1.6485	1.834	1.8484
1.1516	1.4684	1.7947	1.8353	1.8647

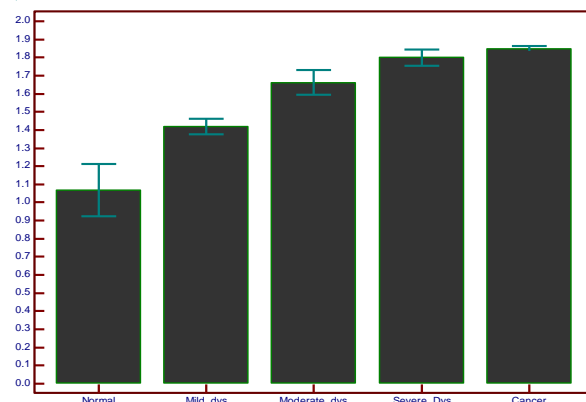
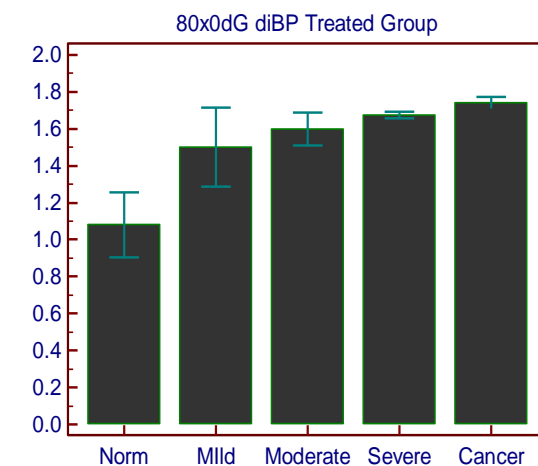


**Table 14: Marker 3: 8-oxo-dG**

Normal	Mild Dysplasia	Moderate Dysplasia	Severe Dysplasia	Cancer
1.2597	1.4011	1.6179	1.6899	1.7206
1.2986	1.5333	1.6362	1.6988	1.7215
1.3336	1.5628	1.6411	1.7013	1.7301
1.3503	1.5052	1.6478	1.7742	1.7788
1.0733	1.5052	1.6079	1.7657	1.7538
1.2534	1.556	1.6986	1.69	1.854
1.2585	1.5676	1.7557	1.6738	1.841



The effect of these markers to increase the precision of the method is studied though a comparison of these 4 markers and FD analysis obtained for each one which was independent of each other (Table 15).

**Table 15: Comparison of markers:**

	MAPK_avg	8-oxodG_avg	PCNA_avg	CD 44_avg
Normal	1.069	1.26	1.283	1.6513
Mild Dysplasia	1.4196	1.51	1.526	1.6522
Moderate dysplasia	1.66	1.64	1.675	1.7466
Severe dysplasia	1.799	1.71	1.742	1.7701
Cancer	1.84	1.759	1.785	1.921

To determine any significant difference between the markers used in the immunohistochemistry techniques, T-tests were done for each of the markers.

**Table 16: Independent t-test for analysis of difference between the effects of markers**

	MAPK- 8oxodG	MAPK- PCNA	8oxodG- PCNA	PCNA-CD44
F-test for equal variances	P = 0.045	P = 0.407	P = 0.971	P = 0.264
Difference	-0.01954	-0.04468	-0.0264	0.146
Standard Error	0.06631	0.1692	0.1276	0.1037
95% CI of difference	-0.15 to 0.11	-0.43 to 0.34	-0.32 to 0.26	-0.093 to 0.38
Test statistic t	-0.295	-0.264	-0.207	1.409
Degrees of Freedom (DF)	58	8	8	8
Two-tailed probability	P = 0.7693	P = 0.7983	P = 0.8413	P = 0.1965

But it was observed that there was no significant difference ( $p>0.05$ ) between any on the markers used.

## **4. DISCUSSION**

### **4.1. Summary of Results**

An experimental controlled OSCC model induced by DBP was used to show that FD analysis is a useful tool to evaluate histopathology changes from normal, different types of dysplasia and OSCC.

1. There can be an increase in accuracy for diagnosis of each histopathology change as we compare each histopathology and add additional pathology based criteria to FD analyses.
2. Evidence was provided that shows FD analysis of experimental derived oral tissues can be reproduced with an in-significant difference between independent investigators with no previous pathology training.
3. The addition of IHC markers, particularly markers that specify basal like progenitor cell populations improve FD analysis.
4. Contiguous sections with IHC can enhance FD analysis.

### **4.2. Innovation**

Pattern recognition based on fractal dimension values was done to understand and predict the progressing stages of oral carcinogenesis. The current method of evaluating cancer tissues is based on training and experience of the pathologist's qualitative predictive behavior. It is often assisted using markers that have varying degrees of quantitative precision. Although consensus conferences are often employed to obtain a diagnosis the underlying approach is not changed from an individual pathologist

evaluation. There are previous publications that identify FD analysis changes in comparisons between normal, premalignant-dysplasia and malignant-OSCC (Cross 1997).

However these specific studies that use FD analysis to focus on oral conditions and still others that focus on other human cancers do not provide any reference or methodology approach to understand the degree of precision and ultimately accuracy for diagnosis (Streba, Pirici et al. 2011).

Moreover, there is to our knowledge no attempt to show how to improve FD analyses in regards to number of sections used, number of areas evaluated, the area of site of evaluation during a comparative study of normal, premalignant and malignant histopathology observations.

Furthermore, other pathology criteria such as, Brandwein's evaluation guide and the WHO squamous intra-epithelial consensus discriminators have again to our knowledge not been used in conjunction with FD analysis to determine whether an improvement to FD analysis accuracy and therefore a general improvement in histopathology diagnostic capability for types of premalignant-dysplasia or between each type and OSCC.

Use of DBP as the carcinogen inducer further contributed to the significance of this study because DBP is a potent environmental carcinogen. The doses used were intentionally low and consistent with human exposure experience to environmental carcinogens of this type. The hamster tumor modeling system is also a standard approach to observe oral carcinogenesis (Schwartz 2000) and offers a continuum of histopathology from normal to premalignant-dysplasia to malignant severity.



One of the more novel attributes examined in this study was the area and density of inflammatory infiltration. This factor is increasingly viewed as significant for understanding oral carcinogenesis (Gimenez-Conti and Slaga 1993). Although we did not dissociate the types of inflammatory cells present through marker characteristics and evaluate function it is interesting to note that a broad overview of this infiltration into epithelial underlying stroma provides relatively quick and low cost criteria for understanding aggressive behavior of OSCC.

In addition, this study included an examination of protein expression and selective cell association with FD patterns. For example we used markers such as PCNA that localizes nuclear change linked to proliferation. This marker identified cells preferentially part of the proliferative zone of oral mucosa in normal, pre-malignant-dysplasia types, and malignant-OSCC. Results from the FD analysis indicated that these cells were significant for the formation of the border that was analyzed for FD. Another marker the CD44 antigen found among stem cell and progenitor keratinocyte populations also located in the stratum basalis enhanced our ability to define the FD border and improve FD analysis. This process was also improved when we compared contiguous tissue sections. This is important because with tissue sectioning part of cells are removed or lost and the tissue can be deformed and contribute to histopathology diagnostic difficulties. Another feature to the IHC presented in this study was the use of general keratinocyte markers such as p38, MAPK and 8-oxo-dG expression. These markers unlike the previous discussed markers will be expressed throughout all layers of the oral mucosa and although enhanced in expression during oral carcinogenesis they do not

provide the specificity and FD analysis improvement found among specific basal and basal –like cell markers.

#### **4.3. Consistency & Repeatability:**

The FD analysis produced similar results when performed by two different individuals using the same tissues for the control animal model study. The software can be reliable when subjected to different pathologists using the same protocols. Usually major error in diagnosis occurs due to difference in predicting the stage of cancer development. This aspect of FD values using Image J software can overcome the drawbacks of a regular qualitative pathological analysis. In addition to giving a quantitative value, it can be repeated to receive consistent values.

Along with fractal dimension values, another pattern recognition feature studied is the lacunarity. This showed a strong negative correlation with the FD values, thus giving more accuracy to the diagnosis. The pathologist can predict different stages of dysplasia with more precision distinguishing mild from moderate dysplasia, severe dysplasia from cancerous tissues. The scatter plot displayed cancerous tissue clusters having high FD value and low lacunarity. The Mild and moderate dysplasia tissues had a comparatively medium FD value when compared to severe dysplasia. This method can be used as a means of standardization of cancer tissues and is a prognostic tool for diagnosis.

#### **4.4. Sensitivity**

A major concern of diagnosis is to differentiate the various stages of dysplasia from Normal and cancerous tissues are overcome by this study. The FD values calculate the histological feature of the tissue and generate a corresponding value, thus giving a value for each stage of cancer development. The T-test carried out between the contiguous stages of cancer proves that they are statistically different giving more precision to prediction. Along with FD values, the inflammatory cells in the infiltrates are used to predict the stage of cancer development. The inflammatory count and the average size of the cells increases with the increase in proliferation of cells. The area of infiltrate increases explicitly at the severe dysplasia tissues where as there is a gradual increase of average count and the size of the cell. This is further used to differentiate and identify the particular stage of cancer progression.

##### **4.4.1. Stem Cell Markers to enhance Sensitivity:**

Sensitivity for this method can be increased by adding stem cell markers to study FD values of the tissues. We assume that with the increase in proliferation in developing the tissues we can predict the presence of progenitor stem cells in the tissues. They are the stem cell markers which have the potential of self renewal and plasticity to differentiate into different types of cells in tumor tissues. So this identification mechanism will help predict the oncogenesis and development of a diagnostic protocol. By incorporating immunohistochemical staining of PCNA markers, we can observe higher fractal dimension values when compared to the tissues without stem cell

markers. The presence of these markers, changes the patterns and the texture of the tissue, thus yielding higher diagnostic sensitivity.

#### **4.4.2. Comparison of Stem cell markers:**

Both proliferating markers (PCNA) and basal cell surface markers (CD 44) were used for staining the tissues to observe which of the markers are more suitable for differentiating the stages of cancer development. T-test was carried out for both the samples, and it was observed that the difference between the two markers was statistically significant, and could indeed be used to enhance the diagnosis. We can confirm the correlation between the markers by carrying out additional immunohistochemical staining of contiguous tissues as discussed above.

#### **4.5. Enhancing Diagnostic tool kit**

Fractal dimension values can be implemented as a diagnostic procedure for oral carcinogenic by incorporating immunohistochemistry methods. Differentiating of normal tissues from dysplasia, mild-moderate-severe dysplasia and OSCC tissues from severe dysplasia can be carried out using this approach. Even though this method is at a very rudimentary stage, it forms the underlying principle for an efficient diagnostic approach to be tested using human tissue sections. This diagnostic tool is enhanced with the use of stem cell markers, to further predict the development of carcinoma. It can also be carried out with different stem cell markers to add precision and increase efficiency to the procedure.

## **5. CONCLUSION**

It can be concluded that through the use of a controlled experimental oral carcinogenesis model, a comparative approach between un-trained investigators, an evaluation for inter-individual variation, inclusion of the aforementioned discriminators such as, POI, Inflammatory infiltrates, Lacunarity, and selection of cell forming the FD analysis border we can assist with standard histopathology to increase accuracy. The use of contiguous tissue was found to increase the precision of FD analysis and overall accuracy thus enhancing the approach to detect histopathological changes. This study proved the consistency of FD analysis using Image J software thus overcoming the drawbacks of a regular qualitative pathological analysis. Various forms of Dysplasia can be differentiated from each other thus displaying increased sensitivity when compared to conventional tissue analysis. This can be enhanced further by using various stem cell markers such as PCNA and CD 44.

## **6. FUTURE AIMS**

We only used a single carcinogen DBP this is a PAH and results we obtained with this carcinogen is expected to be repeated with other PAHs. FD data analysis showing this response can be used as a tool for a wide range of tissues susceptible to cancer development. This study approach can be further continued to human cancer tissues to observe the presence of similar responses as the animal model.

## **7. REFERENCES**

1. (1986). Drinking Water and Health, Volume 6, The National Academies Press.
2. Acin S, Li Z, Mejia O, Roop DR, El-Naggar AK, Caulin C. Gain-of-function mutant p53 but not p53 deletion promotes head and neck cancer progression in response to oncogenic K-ras. J Pathol. 2011 Dec;225(4):479-89.
3. Alonso, L. and E. Fuchs (2003). "Stem cells of the skin epithelium." Proceedings of the National Academy of Sciences of the United States of America 100(Suppl 1): 11830-11835.
4. Baish, J. W. and R. K. Jain (2000). "Fractals and Cancer." Cancer Research 60(14): 3683-3688.
5. Bánóczy, J. (1984). Clinical and Histopathological Aspects of Premalignant Lesions. Oral Oncology. I. Waal and G. B. Snow, Springer US. 20: 3-31.
6. Beachler DC, D'souza G. Oral human papillomavirus infection and head and neck cancers in HIV-infected individuals. Curr Opin Oncol. 2013 Jul 10.
7. Berenblum, I. and P. Shubik (1947). "A new, quantitative, approach to the study of the stages of chemical cartinogenesis in the mouse's skin." Br J Cancer 1(4): 383-391.
8. Brandwein-Gensler, M., et al. (2010). "Validation of the histologic risk model in a new cohort of patients with head and neck squamous cell carcinoma." Am J Surg Pathol 34(5): 676-688.
9. Brandwein-Gensler, M., et al. (2005). "Oral squamous cell carcinoma: histologic risk assessment, but not margin status, is strongly predictive of local disease-free and overall survival." The American journal of surgical pathology 29(2): 167.
10. Brandwein-Gensler, M., et al. (2005). "Oral squamous cell carcinoma: histologic risk assessment, but not margin status, is strongly predictive of local disease-free and overall survival." Am J Surg Pathol 29(2): 167-178.
11. Cheon, D. J. and S. Orsulic (2011). "Mouse models of cancer." Annu Rev Pathol 6: 95-119.
12. Chiang, C. P., et al. (2000). "Expression of proliferating cell nuclear antigen (PCNA) in oral submucous fibrosis, oral epithelial hyperkeratosis and oral epithelial dysplasia in Taiwan." Oral Oncology 36(4): 353-359.
13. Christopher, A. S. and J. K. Mary (2001). "BIOLOGY OF ORAL MUCOSA AND ESOPHAGUS." Journal of the National Cancer Institute. Monographs 2001(29): 7.

14. Cregger, M., et al. (2006). "Immunohistochemistry and quantitative analysis of protein expression." Arch Pathol Lab Med 130(7): 1026-1030.
15. Cross, S. S. (1997). "FRACTALS IN PATHOLOGY." The Journal of Pathology 182(1): 1-8.
16. de Arruda, P. F. F., et al. (2013). "Quantification of fractal dimension and Shannon's entropy in histological diagnosis of prostate cancer." BMC clinical pathology 13(1): 6.
17. Dorne JL, Walton K, Renwick AG. Human variability in xenobiotic metabolism and pathway-related uncertainty factors for chemical risk assessment: a review. *Food Chem Toxicol.* 2005 Feb;43(2):203-16; Long A, Walker JD. Quantitative structure-activity relationships for predicting metabolism and modeling cytochrome p450 enzyme activities. *Environ Toxicol Chem.* 2003 Aug;22(8):1894-9
18. Driemel, O., et al. (2007). "Diagnosis of oral squamous cell carcinoma and its precursor lesions." JDDG: Journal der Deutschen Dermatologischen Gesellschaft 5(12): 1095-1100.
19. Fujita, N., et al. (2002). "Akt-dependent phosphorylation of p27Kip1 promotes binding to 14-3-3 and cytoplasmic localization." J Biol Chem 277(32): 28706-28713.
20. Gimenez-Conti, I. B. and T. J. Slaga (1993). "The hamster cheek pouch carcinogenesis model." Journal of Cellular Biochemistry 53(S17F): 83-90.
21. Giunta, J. L., et al. (1985). "Studies on the vascular drainage system of the hamster buccal pouch." Journal of Oral Pathology & Medicine 14(3): 263-267.
22. Gregory, A. D. and A. McGarry Houghton (2011). "Tumor-Associated Neutrophils: New Targets for Cancer Therapy." Cancer Research 71(7): 2411-2416.
23. Gupta, P. C., et al. (1980). "INCIDENCE RATES OF ORAL-CANCER AND NATURAL-HISTORY OF ORAL PRE-CANCEROUS LESIONS IN A 10-YEAR FOLLOW-UP-STUDY OF INDIAN VILLAGERS." Community Dentistry and Oral Epidemiology 8(6): 287-333.
24. Haas SL, Ye W, Löhr JM. Alcohol consumption and digestive tract cancer. *Curr Opin Clin Nutr Metab Care.* 2012 Sep;15(5):457-67. doi: 10.1097/MCO.0b013e3283566699.; Seitz HK, Meier P. The role of acetaldehyde in upper digestive tract cancer in alcoholics. *Transl Res.* 2007 Jun;149(6):293-7.

25. Hasebe, T., et al. (2005). "Histological characteristics of tumor cells and stromal cells in vessels and lymph nodes are important prognostic parameters of extrahepatic bile duct carcinoma: a prospective study." Human Pathology 36(6): 655-664.
26. Hofman, F. (2001). Immunohistochemistry. Current Protocols in Immunology, John Wiley & Sons, Inc.
27. Kam, Y., et al. (2009). "Nest expansion assay: a cancer systems biology approach to in vitro invasion measurements." BMC Research Notes 2(1): 130.
28. Karperien, A. (1999). "FracLac." V. 2.51e.
29. Karperien, A. (2007). "FracLac for ImageJ—FracLac Advanced User's Manual." Accessible at <http://rsb.info.nih.gov/ij/plugins/fraclac/fraclac-manual.pdf>. Accessed July 21.
30. Kaye, B. H. (2008). A random walk through fractal dimensions, John Wiley & Sons.
31. Krishnan, M. M. R., et al. (2012). "Automated oral cancer identification using histopathological images: A hybrid feature extraction paradigm." Micron 43(2–3): 352-364.
32. Li, C., et al. (2007). "Identification of pancreatic cancer stem cells." Cancer Res 67(3): 1030-1037.
33. Li R, Koch WM, Fakhry C, Gourin CG. Distinct epidemiologic characteristics of oral tongue cancer patients. Otolaryngol Head Neck Surg. 2013 May;148(5):792-6. doi: 10.1177/0194599813477992. Epub 2013 Feb 8
34. Mandelbrot, B. B. (1977). Fractals : form, change and dimension. San Francisco, Freeman.
35. Marshall JR, Graham S, Haughey BP, Shedd D, O'Shea R, Brasure J, Wilkinson GS, West D Smoking, alcohol, dentition and diet in the epidemiology of oral cancer. Eur J Cancer B Oral Oncol. 1992 Jul;28B(1):9-15.
36. McCullough, M. J. and C. S. Farah (2008). "The role of alcohol in oral carcinogenesis with particular reference to alcohol-containing mouthwashes." Australian Dental Journal 53(4): 302-305.
37. Mognetti, B., et al. (2006). "Animal models in oral cancer research." Oral Oncology 42(5): 448-460.



38. Pindborg, J. J., et al. (1985). "SUBJECTIVITY IN EVALUATING ORAL EPITHELIAL DYSPLASIA, CARCINOMA INSITU AND INITIAL CARCINOMA." Journal of Oral Pathology & Medicine 14(9): 698-708.
39. Rahman, S. and A. S. Leong (1991). "Diagnostic immunohistochemistry: current applications and future directions." Malays J Pathol 13(1): 17-28.
40. Raju, B. and S. O. Ibrahim (2011). "Pathophysiology of oral cancer in experimental animal models: a review with focus on the role of sympathetic nerves." Journal of Oral Pathology & Medicine 40(1): 1-9.
41. Rasband, W. S. (2009). "ImageJ, US National Institutes of Health, Bethesda, Maryland, USA." Available at: rsb. info. nih. gov/ij. Accessed 20.
42. Reibel, J. (2003). "Prognosis of Oral Pre-malignant Lesions: Significance of Clinical, Histopathological, and Molecular Biological Characteristics." Critical Reviews in Oral Biology & Medicine 14(1): 47-62.
43. Reiskin, A. B. and R. J. Berry (1968). "Cell Proliferation and Carcinogenesis in the Hamster Cheek Pouch." Cancer Res 28(5): 898-905.
44. Sarstedt, M. and E. Mooi (2010). A Concise Guide to Market Research: The Process, Data, and Methods Using IBM SPSS Statistics, Springer Verlag.
45. Schwartz, J. L. (2000). "Biomarkers and molecular epidemiology and chemoprevention of oral carcinogenesis." Crit Rev Oral Biol Med 11(1): 92-122.
46. Schwartz J, Pavlova S, Kolokythas A, Lugakingira M, Tao L, Miloro M. Streptococci-human papilloma virus interaction with ethanol exposure leads to keratinocyte damage. J Oral Maxillofac Surg. 2012 Aug;70(8):1867-79. doi: 10.1016/j.joms.2011.08.005. Epub 2011 Nov 10.
47. Seitz HK, Stickel F., Acetaldehyde as an underestimated risk factor for cancer development: role of genetics in ethanol metabolism. Genes Nutr. 2010 Jun;5(2):121-8. doi: 10.1007/s12263-009-0154-1. Epub 2009 Oct 22
48. Shafer, W. G. and C. A. Waldron (1975). "Erythroplakia of the oral cavity." Cancer 36(3): 1021-1028.
49. Shklar, G. and J. Schwartz (1993). "Oral cancer inhibition by micronutrients. The experimental basis for clinical trials." Eur J Cancer B Oral Oncol 29b(1): 9-16.

50. Sawair FA, Irwin CR, Gordon DJ, Leonard AG, Stephenson M, Napier SS. Invasive front grading: reliability and usefulness in the management of oral squamous cell carcinoma. J Oral Pathol Med. 2003 Jan;32(1):1-9
51. Singh, B. (2008). "Molecular pathogenesis of head and neck cancers." Journal of Surgical Oncology **97**(8): 634-639.
52. Speight, P. M., et al. (1996). "The pathology of oral cancer and precancer." Current Diagnostic Pathology **3**(3): 165-176.
53. Squier, C. A. and M. J. Kremer (2001). "Biology of oral mucosa and esophagus." JNCI Monographs **2001**(29): 7-15.
54. Streba, C. T., et al. (2011). "Fractal analysis differentiation of nuclear and vascular patterns in hepatocellular carcinomas and hepatic metastasis." Rom J Morphol Embryol **52**(3): 845-854.
55. Tabor, M. P., et al. (2003). "Comparative molecular and histological grading of epithelial dysplasia of the oral cavity and the oropharynx." The Journal of Pathology **199**(3): 354-360.
56. Tanaka, T. and R. Ishigamori (2011). "Understanding carcinogenesis for fighting oral cancer." J Oncol **2011**: 603740.
57. Tanaka, T., et al. (2011). "Oral Carcinogenesis and Oral Cancer Chemoprevention: A Review." Pathology Research International **2011**.
58. Wang, C., et al. (2012). "Evaluation of CD44 and CD133 as cancer stem cell markers for colorectal cancer." Oncol Rep **28**(4): 1301-1308.
59. Wang HT, Weng MW, Chen WC, Yobin M, Pan J, Chung FL, Wu XR, Rom W, Tang MS. Effect of CpG methylation at different sequence context on acrolein- and BPDE-DNA binding and mutagenesis. Carcinogenesis. 2013 Jan; 34(1):220-7. Doi: 10.1093/carcin/bgs323. Epub 2012 Oct 6.; Shen YM, Troxel AB, Vedantam S, Penning TM, Field J. Comparison of p53 mutations induced by PAH o-quinones with those caused by anti-benzo[a]pyrene diol epoxide in vitro: role of reactive oxygen and biological selection. Chem Res Toxicol. 2006 Nov; 19(11):1441-50.]
60. Warnakulasuriya, S. (2001). "Histological grading of oral epithelial dysplasia: revisited." The Journal of Pathology **194**(3): 294-297.
61. Yeh, I. T. and C. Mies (2008). "Application of immunohistochemistry to breast lesions." Arch Pathol Lab Med **132**(3): 349-358.

62. Yadav KS, Gonuguntla S, Ealla KK, Velidandla SR, Reddy CR, Prasanna MD, Bommu SR. Assessment of interobserver variability in mitotic figure counting in different histological grades of oral squamous cell carcinoma. *J Contemp Dent Pract*. 2012 May 1;13(3):339-44
63. Yuspa, S. H. and M. C. Poirier (1988). "Chemical carcinogenesis: from animal models to molecular models in one decade." *Adv Cancer Res* **50**: 25-70.
64. Zach's, Lockshin RA. Cell death: history and future; *Adv Exp Med Biol*. 2008; 615:1-11. doi: 10.1007/978-1-4020-6554-5\_1; Denning DP, Hatch V, Horvitz HR. Both the caspase CSP-1 and a caspase-independent pathway promote programmed cell death in parallel to the canonical pathway for apoptosis in *Caenorhabditis elegans*. *PLoS Genet*. 2013; 9(3):e1003341. doi: 10.1371/journal.pgen.1003341. Epub 2013 Mar 7.]

## VITAE

**NAME:** SREE POORNIMA RAGHURAM

### **EDUCATION:**

#### **Master of Science – Bioengineering**

*University of Illinois at Chicago*

#### **Bachelor of Engineering – Biotechnology**

*Visvesvaraya Technological University, India*

### **EXPERIENCE**

#### **Research Assistant**

##### **Department of Oral Medicine & Diagnostic Sciences**

*College Of Dentistry, University of Illinois at Chicago*

- Analysis of cancerous tissues obtained from the Oral cavity, Head & Neck tissues using ImageJ Software.
- Experience in extensive tissue culture with stem cell markers and immunohistological analysis of the same.

#### **Graduate Teaching Assistant**

##### **Microbiology Lab**

*Biological Sciences, University of Illinois at Chicago*

- Setting up experiments for the laboratory exercises. Outlining the relevant theoretical points and practical procedures for the experiments.
- Responsible for supervision of students during the practical classes in a safe and sterile manner. Assisted in explaining the protocol and clearing of doubts with respect to experiments.

#### **Research Intern, Bioanalytical Lab**

##### **Process Development Plant**

*Biocon Ltd, India*

- Skilled in GC, HPLC (High Performance Liquid Chromatography) HPLC Agilent 1100 series and Agilent 1200 systems Instrumentation and software.
- Carried out experiments involving analysis of pharmaceuticals and bio-molecules using HPLC, UV, IR and downstream processes.

## **PROJECTS**

### **Fractal Dimensional Analysis of Carcinogenic Tissues**

*Department of Oral Medicine & Diagnostic Science*

*College Of Dentistry, UIC*

- Determining the fractal dimensions of oral carcinogenic tissues and stem cells. Culturing Syrian Hamster cells with and observing the stem cell markers in this environment.

### **Bioanalytical Lab - Process Development**

*Biocon, Ltd, India*

- Analysis and Purification of Pharmaceuticals and Biomolecules.
- Effect of varying concentrations of Mobile phase additives on the retention time of Biomolecules.

### **Analysis of Antimicrobial & Phytoremediation properties of Nelumbo nucifera**

*Karnataka State Council for Science & Technology, Indian Institute of Science, India*

- Studied the antimicrobial characteristics of Nelumbo nucifera and its effects on both harmful and beneficial gut flora. Studied the antioxidant characteristics of Nelumbo nucifera.